



Acoustic Emission

A way to stress grade radiata pine

Anders Döhlmark



University of Tasmania
Department of Engineering



University of Tasmania
Department of Engineering



University of Lund
Lund Institute of Technology
Department of Structural Engineering

Acoustic Emission

A way to stress grade radiata pine

by

Anders Döhlmark V-92
710322-3355

Submitted in partial fulfilment of the requirements for the degree of
Master of Science in Civil Engineering
at the University of Lund

University of Tasmania
Australia
January 1997

Preface

This diploma work by Anders Döhlmark has been made to fulfill the requirements for the degree of Civil Engineering at Lund University. The diploma work is formally related to the Division of Structural Engineering of Lund University.

The work has been made at Department of Engineering of University of Tasmania during 1996 under supervision of Prof Peter Doe, who also evaluated the thesis. Many thanks are due to Peter Doe for his assistance.

In addition, the thesis has been evaluated at the division of Structural Engineering for fulfilment of the degree.

Lund March 1997

Sven Thelandersson
Professor of Structural Engineering



Summary



Summary

This research was undertaken at the University of Tasmania. The radiata pine for the tests was provided by Auspine's sawmills in Scottsdale in Tasmania and Tarpeena in South Australia. The tests followed the procedure set out in the joint Standards Australia / New Zealand, AS / NZS 4063:1992, for in-grade strength and stiffness evaluation.

Acoustic emission is the response to the application of stress. Two sensors were attached to the setup to measure acoustic emission as a voltage. The beams were loaded until rupture in four point bending. LabVIEW® continuously took readings of load, deflection, acoustic emission, date and time and saved all data on a hard drive.

The acoustic emission for all sticks were transformed into a representative stick. At around 80% of ultimate load, corresponding to 0.5-0.6V, there was an increase in acoustic emission. The pattern of acoustic emission for each stick was divided into three types, depending on at what percentage of ultimate load the acoustic emission reached 0.6V. The limits were less than 50%, 50-90% and more than 90%. The majority were in the range 50-90%, but 15% actually failed without any warning.

From the representative stick it was derived that the theoretical slope of ultimate reading to the reading when the acoustic emission reached 0.6 V was 1.212. The tests gave a slope of 1.384. The hypothesis that the theoretical slope and the slope from the tests were the same and that the difference was caused by random error could not be rejected at a confidence level of 90%, which is more than acceptable. Acoustic emission and Modulus of Elasticity were compared in their ability to predict strength. The correlation for acoustic emission was much better.

Acoustic emission has proven to be a good way to predict the strength of radiata pine. A significant increase in the ratio of acoustic emission to load took place at 80% of ultimate load. At this early stage though there was a remarkable high wastage of beams failing without warning. The relationship between acoustic emission and ultimate load is much better than the relationship between Modulus of Elasticity and Modulus of Rupture, which the mechanical stress grading system is based on.



Acknowledgments



Acknowledgments

I would like to send all my gratitude and appreciation to all people who have contributed in one way or the other to the completion of this thesis.

Special recognition to

Associate Professor Peter Doe, supervisor. Thanks for your enthusiasm and for always having time to share that enormous amount of knowledge of yours. Thankyou for your initiative to the exchange between University of Tasmania and University of Lund.

Associate Professor Annika Mårtensson. Thanks for your support and giving me the opportunity to broaden my horizon.

Professor Sven Thelandersson for his home-ground support.

Daniel Niechoda hardware and software guru.

Alan Belle, Dean Chatwin and Adam Redman, fellow engineers, for their assistance and good company.

Drew Honeychurch, the best mate to break radiata pine with.

Rob Wrigley, handyman.

Research Officer Gregory Nolan for his LabVIEW skills.

Auspine for providing the radiata pine and their helpful Quality Managers Mr Pluck-Hahn and Mr Styles.

My family and friends for their long distance encouragement.



Contents



Contents

1. Introduction	1
2. Wood	2
2.1 Wood as a material	2
2.1.1 The structure of wood	2
2.1.2 Hardwood and softwood	3
2.2 Australian forests	3
2.2.1 Short history	3
2.2.2 Radiata pine	4
3. Acoustic emission	8
3.1 Description	8
3.2 The use of acoustic emission	8
3.2.1 The application for wood	8
3.3 How the sensors work	8
3.4 The sensors used for this research	9



Contents



4. LabVIEW	11
4.1 Introduction to LabVIEW	11
4.2 LabVIEW in this research	11
5. Population and samples	12
5.1 Scottsdale and Tarpeena	12
5.2 Selection of samples and marking	13
6. Four point bending test	15
6.1 The setup	15
6.2 Calibration	17
6.3 The testing	18
6.4 Problems and solutions	20
6.5 Saving the data	21



Contents



7. Analysis of the test	22
7.1 Rejection of samples	22
7.2 Sample distributions	22
7.3 AE2 Max analysis for Tarpeena	25
7.3.1 First support for the theory	25
7.3.2 Different patterns	28
7.3.3 Statistics of the analysis	30
7.3.4 Comparison between AE2 Max and MOE to predict strength	34
8. Conclusions	36
Appendix A Beam test 2-3.vi	
Appendix B Comparison between AE1 and AE2	
Appendix C Explanation of the data	
Appendix D Data used in the analysis	
References	



Introduction



1. Introduction

This thesis was accomplished from September 1996 to January 1997 as part of my Master of Science in Civil Engineering at the University of Lund. Thanks to an exchange initiated by Associate Professor Peter Doe and Associate Professor Annika Mårtensson I had the opportunity to undertake this thesis at the University of Tasmania.

The common machine stress grading system, where a constant relationship between Modulus of Elasticity and Modulus of Rupture is anticipated, is not very reliable. This raised the question of a better way to stress grade timber. Acoustic emission has proved to be a good method to predict the strength and monitor drying of hardwood. Little research on acoustic emission as a way to predict the strength of softwoods has been made. Radiata pine is one of the most common softwoods used for construction. The scope of this research has been to see if radiata pine can be stress graded with the use of acoustic emission.



Wood



2. Wood

2.1 Wood as a material

2.1.1 The structure of wood

Like all living things trees have developed through evolution to become specialists in what they do. The root system has to provide the tree with nutrition and it has to supply support so that the tree will not fall over. The tree trunk must be able to transport the essentials for the tree, as well as it has to carry its own weight, snow and cope with wind. The function of the crown of the tree is to expose the leaves or the needles to facilitate photosynthesis. The structure of wood has developed to meet these demands.

Wood is a very nonhomogeneous material. Its properties vary substantially with its three principal axes. These are longitudinal (along the growth rings), radial (across the growth rings) and tangential (parallel to the growth rings), see Figure 2.1. In the middle of the

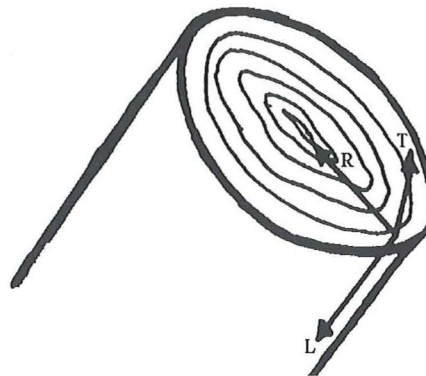


Figure 2.1

The three principal axes for wood: L longitudinal (along the growth rings), R radial (across the growth rings) and T tangential (parallel to the growth rings).

tree is the heartwood. The heartwood is darker than the sapwood around it. There are significant differences between the two. The heartwood does not have any living cells in contrast to the sapwood, which does have living cells. New sapwood is formed when the tree grows. When the cells die they turn into heartwood. The change in colour comes from the deposition of extraneous materials in the cell cavities (1). Although there might be a slight change in density, there is no difference in strength between heartwood and sapwood. The major distinction is the durability, where the heartwood has more protection against fungi, decay and insects, due to the contents of foreign materials.



Wood



2.1.2 Hardwood and softwood

There are three main constituents for wood. Cellulose works as the skeleton. The hemicellulose is the tree's matrix and lignin is like glue to bind the cells together (2). Wood is classed as either hardwood or softwood. The names are not really well thought out, as there are quite soft hardwoods and relatively hard softwoods. The distinction lies in the cell structure, see Figure 2.2. The distinguishing feature for hardwood are the large

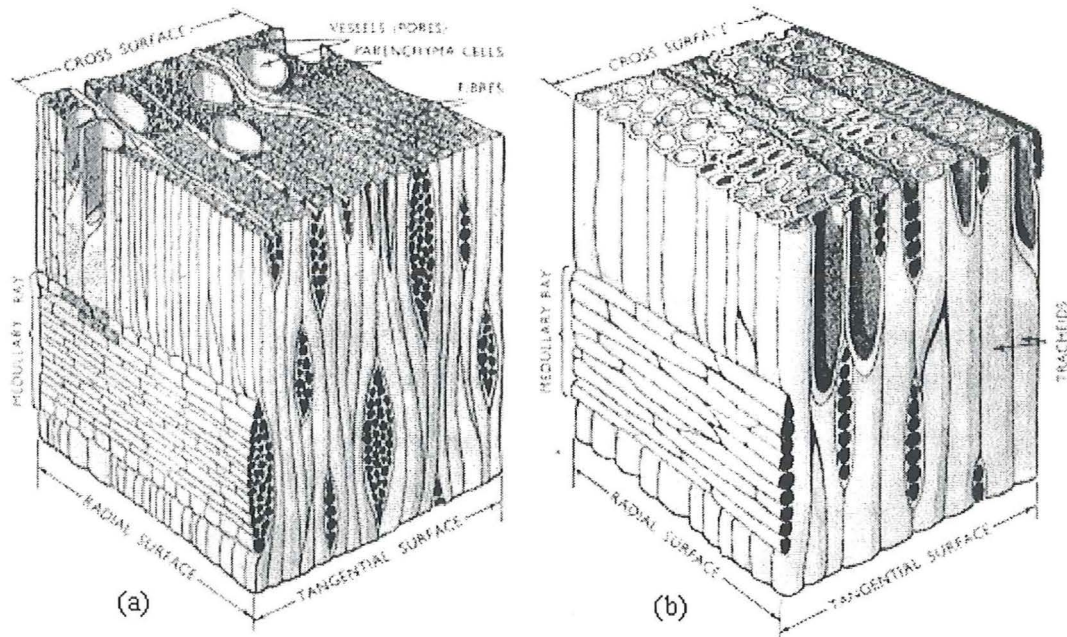


Figure 2.2

The highly magnified blocks of wood represents (a) hardwood and (b) softwood. The characteristic for hardwood are the large vessels or pores, which are absent in softwood (1).

vessels or pores, which can not be found in softwood. Hardwoods can be found in both tropical and temperate zones, while softwoods are only common in temperate regions. Because of this there are a lot more different species among the hardwoods than the softwoods. The softwoods are much more uniform in their structure, in contrast to hardwoods, where the trained eye visually can distinguish different species. It is hard to by eye separate one softwood from another. As the hardwoods show a wider structural variation they have a greater range in physical properties like permeability and capillarity.

2.2 Australian forests

2.2.1 Short history

Before the first European came to Australia about 10% of the continent was covered by forest. The settlers immediately started to make use of it. Timber was felled to build



Wood



houses and land cleared for agricultural needs. Wood was also the main resource for a lot of industries like ship yards and paper mills.

In 1795 the first regulation was issued to protect the stands of cedar. The years to come several laws followed to control the cutting of timber. The first step toward commercial forestry came in 1871, when the New South Wales government set aside Crown Lands to grow hardwood (3). Australia has a lot of hardwoods, like eucalypts, oak, maple and acacia, but there is a shortage of native softwood suitable for timber production. To increase growth, production and revenue several states tested different native and imported species by the end of the nineteenth century. One of the most successful was *Pinus radiata*.

2.2.2 Radiata pine

Radiata pine, see Figure 2.3, is native to southern California. It has been introduced to several countries, like Australia, New Zealand, Chile and South Africa. It is the most often planted softwood in both temperate and warm regions. Radiata pine made its first

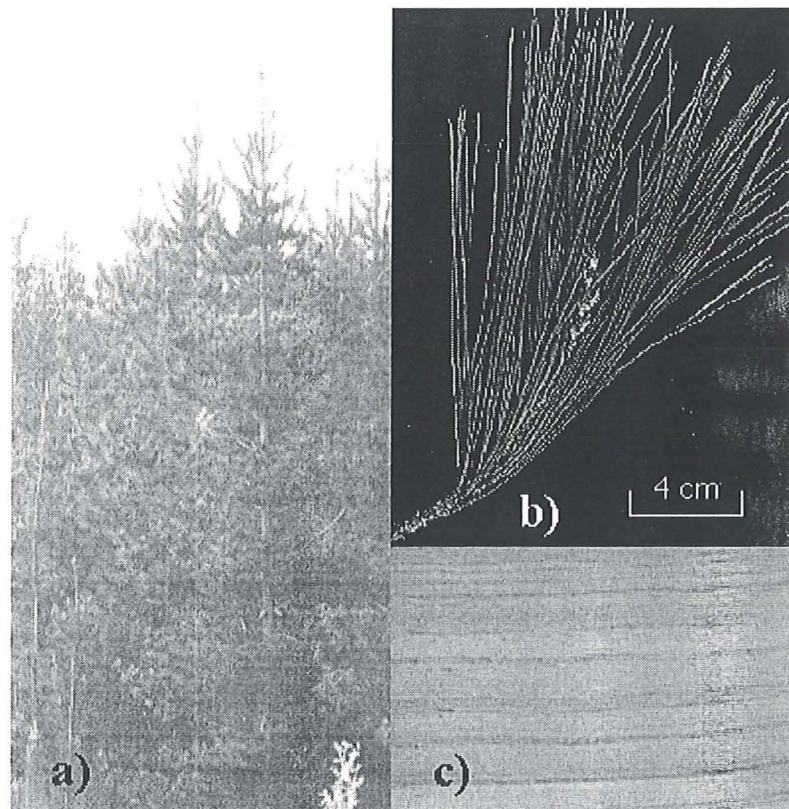


Figure 2.3
In a) is radiata pine as it grows in a forest (4). A close up of the needles is found in b) (5). A sawn piece of radiata is shown in c) (6).



Wood



appearance in Australia when it was planted for forestry at Bundaleer, in the mid-north of South Australia, in 1876 (3). The introduction of radiata has been successful, as you can see in Table 2.1, with 720,000 ha of plantation in 1993. That means that about $\frac{3}{4}$ of the

	NSW ha	Vic ha	Qld ha	WA ha	SA ha	Tas ha	NT ha	ACT ha	Aust. ha
Pinus radiata	250050	212103	3381	60670	104128	76130	-	14136	720598
Pinus elleottii	4785	3	70029	210					75027
Pinus pinaster	71	1218	-	27080	2479	5	-	-	30853
Pinus caribaea	60	3	52747	10			2602		55422
Araucaria spp.	1647	-	45479	-	-	-	-	-	47126
Other	9407	2017	16995	660	341	297		408	30125
Total	266020	215344	188631	88630	106948	76432	2602	14544	959151

Table 2.1
Softwood plantation in Australia in 1993 (3).

softwood plantation are radiata. The plantations are mainly in areas with rainfall above 650 mm. The point of view has been that this is necessary for the plantation to yield well. In such zones radiata grows at an average of 20-23 m³ / ha per year (5). The growing of pine on plantations does not cause excessive damage to the soil. Pine plantation results in less damage to the environment than most other kind of modern agriculture, as it does not use as much chemicals. Native forests can grow well on former pine plantation land.

Favourable soil for radiata are coarse soils, usually sandy loams. The trunk is straight and it grows to a height of about 15-30 m and the diameter is about 30-90 cm. In somewhat 20 years radiata can reach mature size (6). In general radiata is straight grained, but it may contain spiral grain. The heartwood, which usually is pink-brown in colour, has little resistance to fungi, decay and insects. The colour of the sapwood is normally pale.

Timber can be sawn in a number of ways. Backsawn, also called slabsawn or plainsawn, is sawn so that the growth rings are inclined at less than 45° to the wide face. Quartersawn, or edge-grained sawn, is when the timber is sawn so that the angle between growth rings and the widest face is greater than 45°. In Figure 2.4 you can see how backsawn and quartersawn timber differs from each other.



Wood

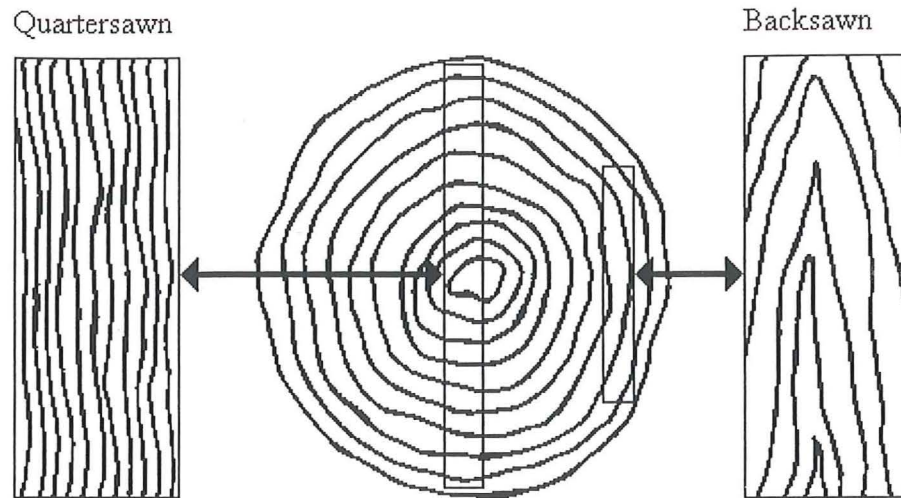


Figure 2.4
Backsawn and quartersawn timber after idea from (7).

Seasoning of radiata can be carried out quickly with a temperature of 120-130°C. When wood dries it shrinks. Characteristic cross-sectional dimension in relation to seasoning changes are shown in Figure 2.5. The effect of dimensions because of seasoning is quite modest when it comes to radiata.

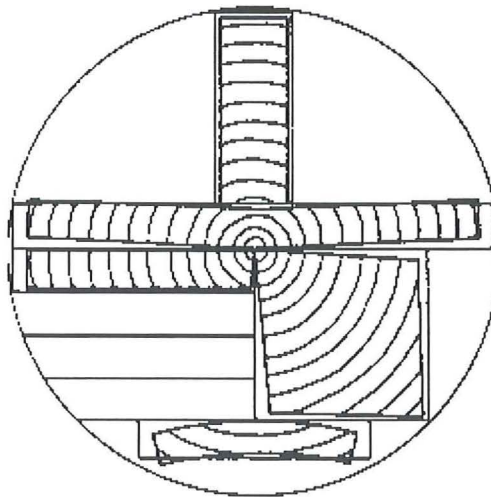


Figure 2.5
Characteristic cross-sectional dimensions in relation to seasoning for sawn timber with different location in the log (8).

Timber used for construction has to be stress graded. Most countries have their own rules when it comes to stress grading of timber. Australia follows Australian Standard. Timber



Wood



can be classified by three methods. Two of them, visual and mechanical, are non destructive. The Modulus of Elasticity (MOE) is measured at a relatively low load. The wood is also visually checked for knots and other defects. By visual inspection and the assumption of constant relationship between stiffness and ultimate strength it can be classified into the right strength group. The method is not particularly good. The third method called proof grading is partly destructive. When proof grading the wood is loaded to a particular load. It is then obvious that it will manage to take that load and the timber can be graded. There is though a lot of waste connected with proof grading, as some pieces will not manage the proof load.

Strength properties are rather low for radiata. Factors like that radiata on plantations grow fast and that the wood contains quite a lot of knots lower the ability to take load. In Australian Standard, AS 1720.1-1988, sawn structural timber is classified into 12 stress grades, F2 to F34. The number in the F-system corresponds to the basic working stress in MPa (9). Seasoned radiata pine is stress graded F5-F14. It seems modest when you compare with Australian hardwoods, which are stress graded up to F34.

Radiata pine is used in a number of ways. Wildlife and recreation make use of it as well as the forest industry, which main products from radiata are sawn timber, plywood, pulp, posts and export woodchips



Acoustic emission



3. Acoustic emission

3.1 Description

“An acoustic emission is a sound wave, or more properly, a stress wave that travels through a material as the result of some sudden release of energy in the material due to the application of stress” (10).

When we expose a structure, or like in this research a wooden beam, to stress we can not actually hear the stress, but we can hear the result of it. For wood the stress will make the fibres to slide against each other and this will be heard as a crack. The crack is the acoustic emission, AE, in consequence of the applied stress. AE can be measured and recorded with the right equipment.

3.2 The use of acoustic emission

The main use for AE is to detect micro cracks or slips in the crystalline component (hemicellulose) of the wood. This will give an idea on the condition of a structure and will reveal faults before they cause structural damage. There are sensors specially designed to work under water. They can for instance be used on submerged structures. Airborne sensors can be used in pressurised spaces like an aircraft. Rolling sensors make it possible to measure AE on a continuous basis.

3.2.1 The application for wood

There are two primary applications for AE that are special for wood. It can be used to control the seasoning of timber and serve as an additional way to stress grade timber products. Associate Professor Peter Doe and his team at the University of Tasmania have for several years researched the use of AE as a control mechanism in timber seasoning technology. It has been known for many years that there is a relationship between AE and strength. Adams (11) found that there was a distinct increase in AE as the wood went from the elastic to the plastic area in the stress versus strain diagram. When it comes to stress grading a lot of research has been conducted at the Tokyo University of Agriculture and Technology. AE is found to be an effective method to evaluate wood for knots. Sato et al (12) concluded that even at a low bending stress level many AE signals were generated around knots. A combination of AE and measurement of MOE was later used to stress grade boards. AE has the advantage that it can be used to detect compression failures, which can not be done by the MOE.

3.3 How the sensors work

The sensors, or transducers, used to registrar AE are very sensitive microphones, which will turn the sound into an electric signal. The sensors, see Figure 3.1, rely on the piezoelectric effect. The piezoelectric effect is when pressure is applied to a crystal an



Acoustic emission



electric field will develop. In the same way will an electrical field cause mechanical deformation.

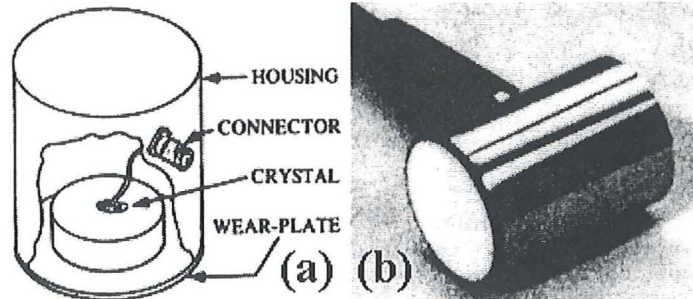


Figure 3.1

In (a) is the interior of the transducer. The pressure on the wear-plate turns into an electric signal by the crystal. In (b) the transducer is shown from outside facing the wear-plate (13).

Loading the beam will consequently give a toning sound wave. When the sound wave hits the wear-plate it will cause the wear-plate to vibrate. These extremely small vibrations apply pressure to the crystal, which in turn converts the pressure into a voltage. This voltage is amplified and fed into a counting circuit. Depending on the type of sensor the time interval for counting the crystal's vibrations can be set from parts of a second up to many seconds. Within the interval the counter counts the number of crystal vibrations with a greater amplitude than the set threshold. The so called sample and hold function "remembers" the counts from previous time intervals. A digital / analog converter generates a DC-voltage, which is proportional to the number of acoustic events. This voltage is thus a measure of the AE and hence the stress.

In this research the time interval was set to 2 seconds. The AE was registered when the load got up another 0.20 kN. This usually took about 6-8 seconds. This means that in general 3-4 time intervals elapsed between each reading. The hold function stored the count rate for each completed time interval. The counts for the latest completed time interval at the time for a reading equals the AE for that reading. The maximum AE between two readings is given by the highest number stored in the sample and hold function.

3.4 The sensors used for this research

The sensors are manufactured by Physical Acoustics Cooperation, PAC. The sensor model used is called R6I (60 kHz, 40 dB). It is a standard R6 sensor with a low-noise Field Effect Transistor (FET) input 40 dB preamplifier integrated in the stainless steel case. The crystal is completely enclosed for Radio Frequency Immunity (RFI) and Electro Magnetic Immunity (EMI). This makes it possible to have long cables without the need for separate preamplifiers. The sensor drive capability for the R6I is up to 1000 m. The features for model R6I are gathered in Table 3.1.



Acoustic emission



R6I	
Dimension DIA x HT (mm)	29 x 40
Weight (g)	98
Operating temperature (°C)	-45 to +85
Shock limit (g)	500
Case material	Stainless steel (304)
Face material	Ceramic
Connector type	BNC

R6I	
Connector location	Side (3)
Peak sensitivity Ref V/(m/s)/ [Ref V/mbar]	120 [-26]
Operating frequency range (kHz)	40-100
Resonant frequency (kHz)	50 [90]
Directionality (dB)	±1.5
Grounding	B
Seal type	Epoxy

Table 3.1
The features of Physical Acoustics Corporation's AE sensor model R6I (13).



LabVIEW



4. LabVIEW

4.1 Introduction to LabVIEW

LabVIEW® (Laboratory Virtual Instrument Engineering Workbench) is a software product of National Instruments. It makes it possible to register the real events during the experiment on your computer screen. By turning the real physical happening, like load or deflection, into a voltage it can be analysed by the computer. To do this you must have a Data Acquisition (DAQ) so the computer will be able to evaluate the signals with the Virtual Instrument (VI) programmed for the experiment. The use of LabVIEW goes far beyond the fact that you can gather all the gauges for the experiment on the computer screen. LabVIEW is most certainly a powerful tool to monitor, evaluate, transform and visualise data from a test.

You can visualise results in a variety of gauges, plot them in a number of graphs and save them to a file. The time and date for each measurement can be added. Arithmetic, trigonometric and logarithmic functions as well as statistical and comparison functions are just some of all the available features in LabVIEW.

With the graphical program language “G” you make the VIs using a block diagram approach. Icons represent the different functions in LabVIEW and they are connected using a “wire”, which indicates the flow of data in the block diagram. In this way you can use all the features in LabVIEW and wire them to suit your needs best. The block diagram is later on compiled by LabVIEW into machine code. When you run the program you will see the Front panel with its input set by the operator and the output resulting from the VI.

4.2 LabVIEW in this research

LabVIEW was used in this research to register load, deflection, current AE and maximum AE for each load step, date and time. All the data were saved to file to be evaluated later on. Load, deflection and current AE together with the duration of the single test were simultaneously displayed on the computer screen. This made it easier to keep track of the wanted load rate. The AE gave an indication when the beam was about to break.

The VI used in the start was called Beam test 2-2.vi. It was created by Research Officer Gregory Nolan at the Department of Architecture at the University of Tasmania. It took us quite some time before it was discovered that the program failed to register the maximum AE and the load was only recorded at the load step. More about this and its consequences in 6.4 Problems and solutions. After a lot of thinking Mr Nolan finally was able to find the error, which I corrected in the next version Beam test 2-3.vi. In Appendix A is a more thorough description of Beam test 2-3.vi.



Population and samples



5. Population and samples

5.1 Scottsdale and Tarpeena

The material which was tested for this research was radiata pine provided by Auspine's sawmills in Scottsdale in Tasmania and Tarpeena in South Australia. The radiata pine accessible to the respective sawmill is that sawmill's population. From each population a sample was drawn to be tested. A sample is any portion of a population.

There are some differences in the growing conditions at Scottsdale and Tarpeena. The sawmill in Tarpeena takes all the radiata from Auspine's own plantations in South Australia, while the Scottsdale sawmill gets its radiata from different cultivators in Tasmania. The conditions for the radiata is therefore probably more homogenous for the Tarpeena samples.

In the climate of South Australia radiata will grow faster than in Tasmania. From this it is expected that the Tarpeena samples will reach cutting size earlier than the Scottsdale samples. According to Quality Manager Mr Pluck-Hahn at Tarpeena their trees are cut at an age between 18-35 years. Quality Manager Mr Styles at Scottsdale said that the Tasmanian radiata were cut at an age of about 30 years. As the strength usually is higher for a slow growing tree it is also likely that the radiata from Scottsdale will be stronger on average.

When the logs come to the sawmill they are sorted by size, into small and large logs. They are then sawn in sawing patterns that will give as much as possible out of the log. The different dimensions are then sorted and taken to dry in the kiln for 12 h at 130°C. After drying in the kiln the moisture content is 8-15 %. Another 10 h is needed for stress relaxation after the drying. Then it is time for the stress grading. The stress grading machine works at a speed of about 120 m per minute. The beams are loaded in the machine to measure MOE around the minor axis, see Figure 5.1. From MOE the strength is extrapolated and the grading is marked in colour on the stick. The machine stress grading is followed by a visual grading, as the machine does not consider the ends of the beam. Those beams which meet the visual inspection are marked with their corresponding F-grading.



Population and samples

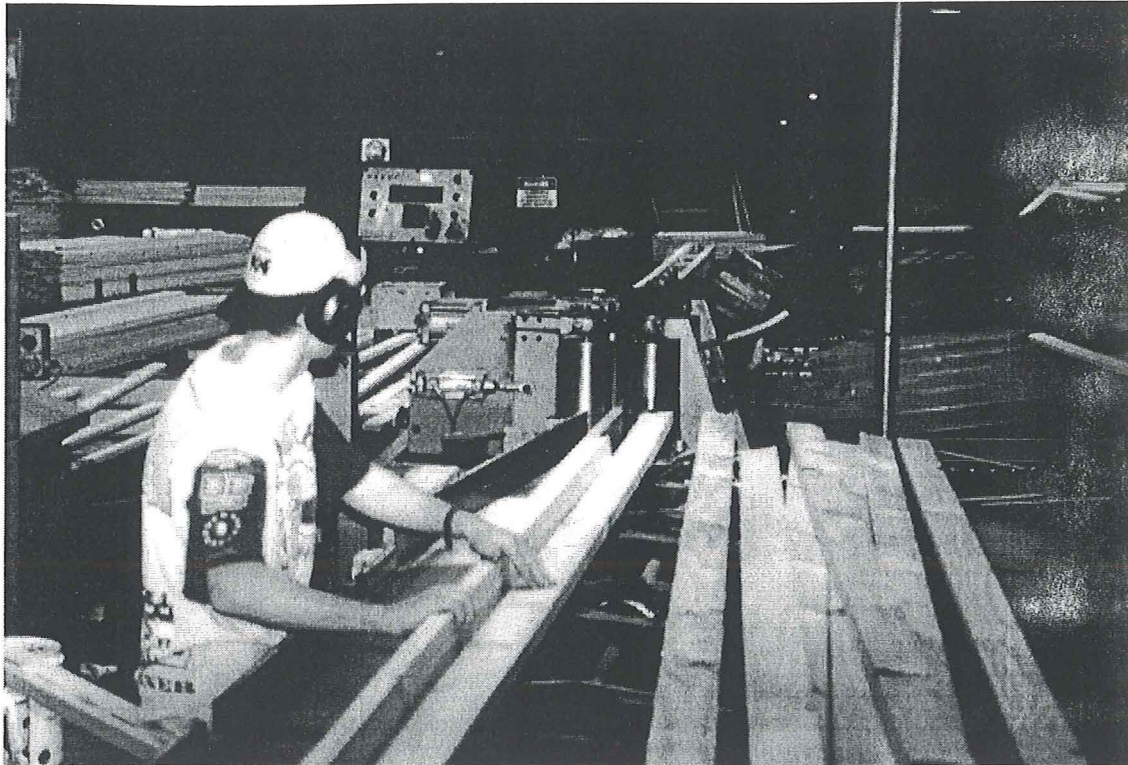


Figure 5.1
Mechanical stress grading at Auspine's facility at Scottsdale, Tasmania. The stress grading is derived from the measurement of MOE around the minor axis.

5.2 Selection of samples and marking

The intention was to get random numbers from a computer to select the samples. That turned out to be non-practical from a production point of view. Therefore the selection was made on a time basis. After the sticks had been finally graded one was taken every five minutes.

The research on the acoustic emission was completed together with the Auspine In-Grade Pilot Study, which was carried out by P.J Yttrup & Associates Pty. Ltd. The scope of an in-grade study is to evaluate structural properties of graded timber and verify the accuracy of grading techniques. The tests carried out in this research followed the procedure set out in the joint Standards Australia / Standard New Zealand, AS / NZS 4063:1992 , for in-grade strength and stiffness evaluation. The samples from Scottsdale and Tarpeena were tested for four point bending, shear, tension and compression along and across the grain. The samples came to the testing facility at the University of Tasmania in two different lengths, 3300 mm and 4500 mm. The cross section, breadth x depth (b x d) was 35 x 90 mm. The sticks were marked with "Top", "S" for Scottsdale or "T" for Tarpeena and numbered. The 3300 mm sticks were used for the four point bending test, compression test along and across the grain, moisture content and density. They were numbered S71-



Population and samples



S140 and T101-T200, while the 4500 mm sticks, that would be used for tension test, shear test, moisture and density, were numbered S1-S70 and T1-T100.

Each stick was sawn in the lengths shown in Figure 5.2 and every piece was marked with "Top", the same number as the stick it was sawn from, and a letter A-D. The letters indicated in what test the piece was going to be used for. For the 3300 mm sticks "A" was for four point bending, "B" for moisture and density, "C" for compression along the grain

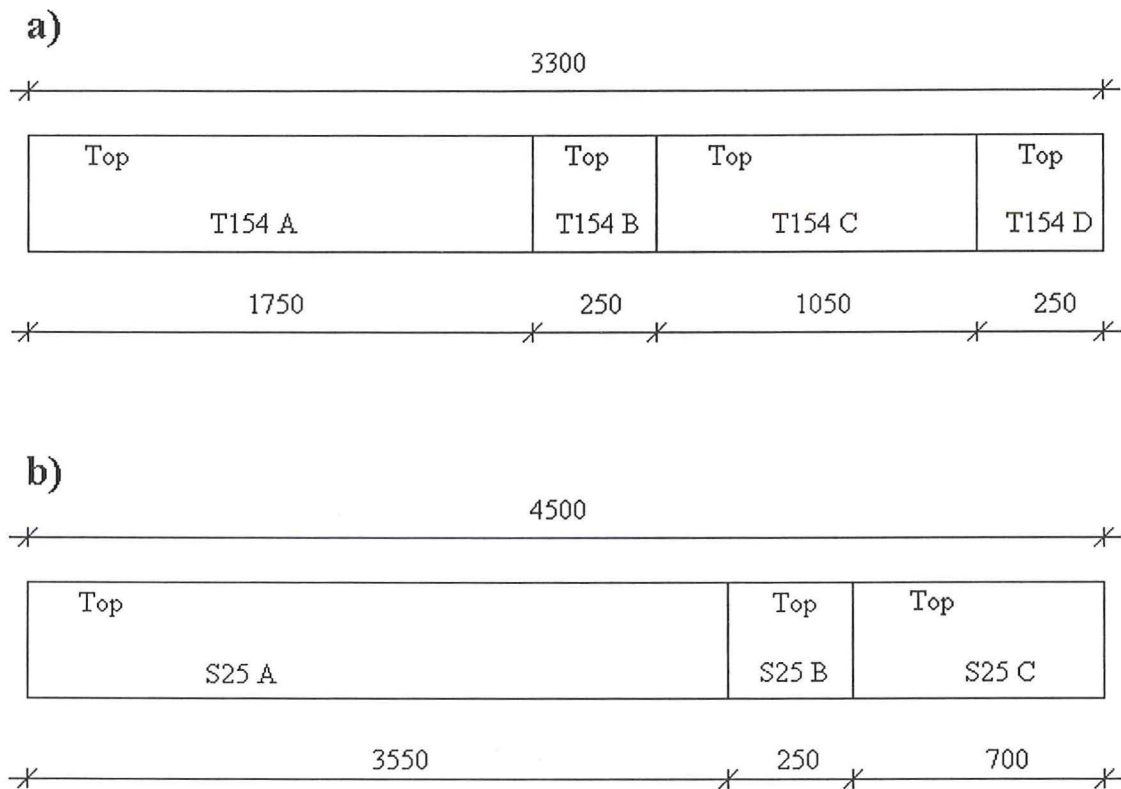


Figure 5.2

The lengths in which the sticks were sawn and the marking of two of them. The other sticks were marked in the same way, except for the number which is individual. The 3300 mm sticks in a) were used for four point bending marked "A", moisture and density "B", compression along the grain "C" and compression across the grain "D". The 4500 mm sticks were used for tension marked "A", moisture and density "B" and shear "C".

and "D" compression across the grain. For the 4500 mm sticks "A" was for tension, "B" for moisture and density and "C" for shear. The letters A, B, and C are all used twice, but there was no risk for a mix up since the numbers differ. Except for those with a "B" there was also a difference in length. For instance S78 B is the Scottsdale moisture and density piece from the 3300 mm stick.



Four point bending test



6. Four point bending test

6.1 The setup

The test was performed at the testing facility of the Department of Architecture at the University of Tasmania Launceston campus. By the time it was decided to collect the AE data from the same samples as the Auspine In-Grade Pilot Study the setup had already been made by Mr Drew Honeychurch. Except for the AE we were ready to go. The final setup is seen in Figure 6.1.

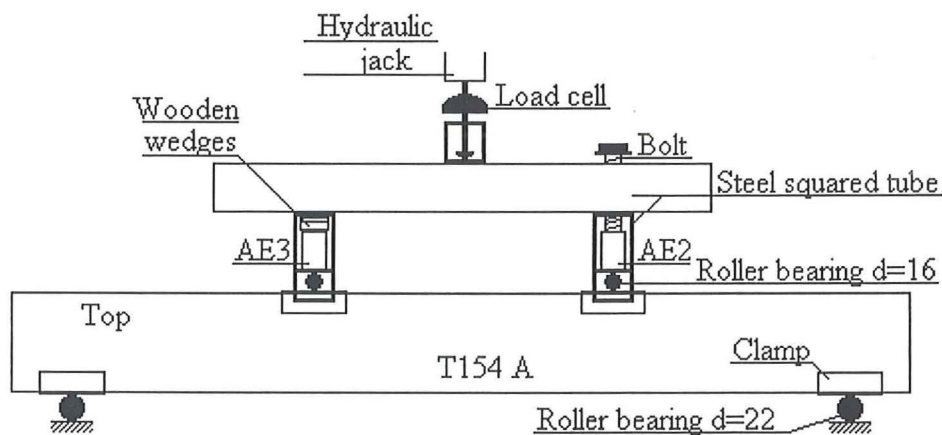


Figure 6.1
The final setup for the four point bending test.

The hydraulic jack pressures on the steel squared tube. The load cell in between, model 1210-AJ from Interface, gives the corresponding load as a voltage. The load goes through the tube and the steel housing to the roller bearings. The clamp under the roller bearing will spread the force on 74 mm of the beam's breadth. It is supposed to be a point load, but the concession to spread the load slightly was necessary to prevent local crushing under the load point. The microphones were placed in the housings right over the load point. To assure sufficient acoustic coupling between the face of the sensor and the metal surface, grease was applied under the wear-plate. For AE2 a spring and a bolt helped to keep it in place and gave a light pressure against the metal. For AE3 the same result was achieved with a spring and two wooden wedges. The free body diagram and the measurements, according to AS / NZS 4063:1992 (14), for the setup is shown in Figure 6.2.



Four point bending test

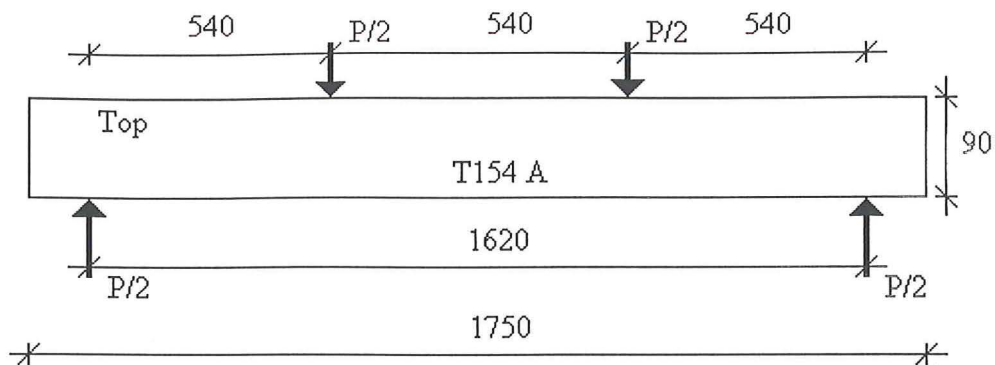


Figure 6.2
The free body diagram and the measurements for the setup.

To start with we had a different approach where to place the AE sensors. It was desirable that the AE sensors got good contact with the beam. A clamp, see Figure 6.3, was made by Mr Rob Wrigley to attach the sensors, AE1 and AE3, to the beam. When the sticks broke there was a big bang and often the beam got splintered causing great pressure

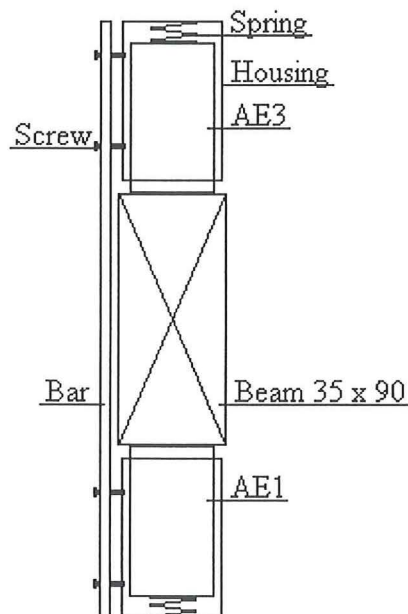


Figure 6.3
The clamp used to attach the sensors AE1 and AE3 to the beam

against the microphones and the bar, which became warped. The clamp was tied with a rope to stop it from falling to the floor when the beam broke. The strain for the sensors turned out to be severe. The top of the case of the sensors was damaged and the signals



Four point bending test



from AE3 started to look strange. Ten sticks were broken before the test procedure was reviewed. As we could not continue destroying microphones we had to come up with another solution. From the start one microphone, AE2, had been attached to the steel bar right over the point where the load got to the beam, see Figure 6.4. This was to see if the AE could be recorded without the actual sensor in direct contact with the wood.

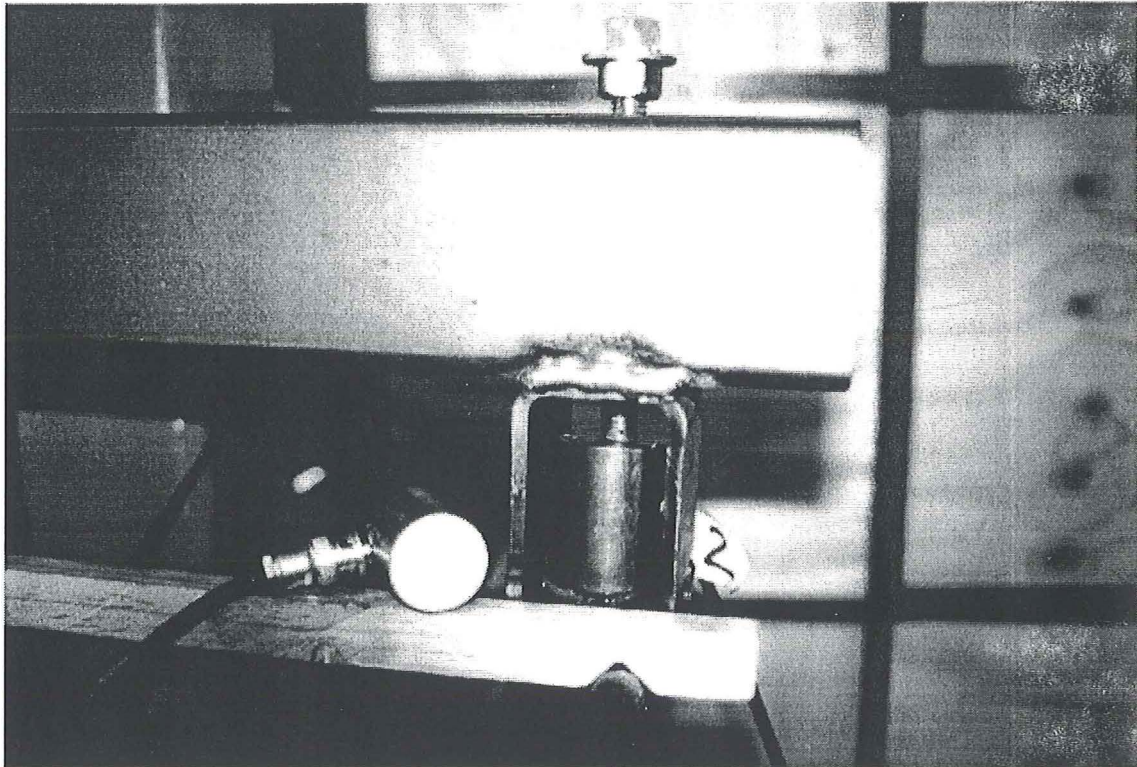


Figure 6.4
AE2 in its location right under the load point. A screw acting on a spring holds the sensor in place. To the left is another sensor showing the wear plate.

When comparing the results from the AE achieved from the sensors on the beam and the one on the steel bar, we found the pattern to be the same, see Appendix B. Therefore it was decided not to use the microphones on the stick. Instead we relied on AE2. To get as much data as possible from the test AE3 was moved from the clamp and attached to the steel bar right over the other load point.

6.2 Calibration

The load cell was calibrated using a steel ring and a pressure gauge, see Figure 6.5. The voltage from the load cell is turned into a numeric value in Pressure per Square Inch (PSI) on a separate display and sent to the DAQ. At several different loads the numeric value was compared with the reading of the pressure gauge to calibrate the voltage input to the DAQ.



Four point bending test

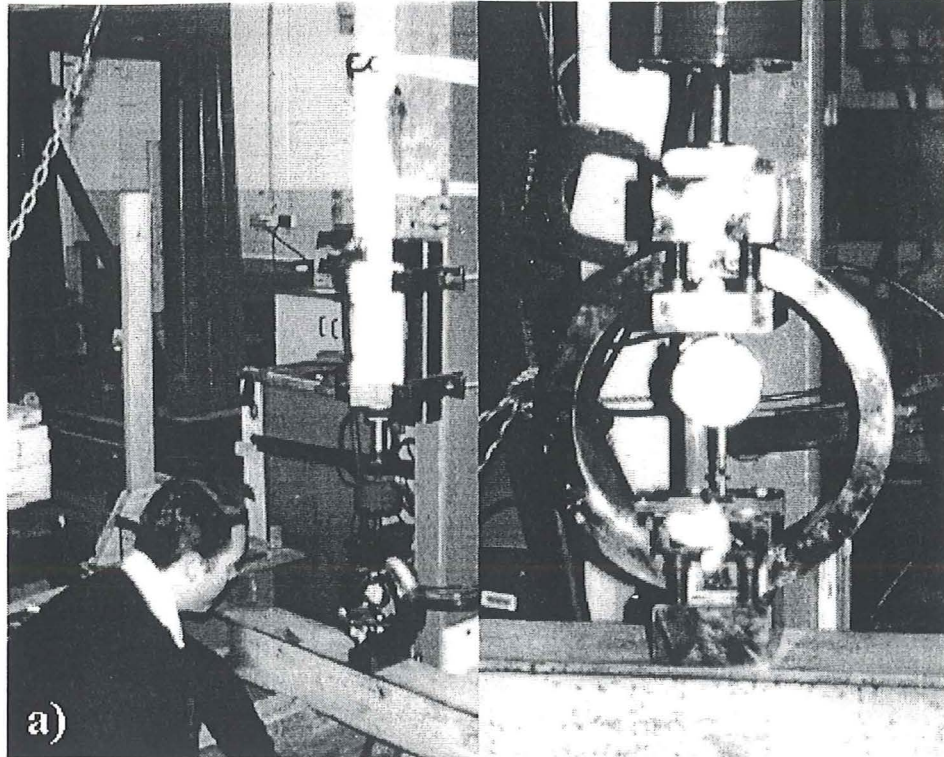


Figure 6.5

In a) is the calibration of the load cell using a steel ring and in b) is a closer look at the steel ring and the pressure gauge.

The AE was measured as a voltage for relative comparison of the signals. As it is beyond the scope of this research to give an absolute value between AE and load, there was no need for calibration of the sensors. The important thing was that the adjustments for each sensor stayed the same throughout the testing, so relevant relative comparison could be done. The count rate was set to 2 s. The threshold for AE3 was set considerably higher than for AE2. This was made to see if blocking of small AE and background noise would be a better way to go. That evaluation has to be done another time though.

6.3 The testing

The testing was done together with Mr Drew Honeychurch. Above in Figure 6.1 is a picture of the setup and in Figure 6.2 is the free body diagram with measurements. The test of each stick was divided in two parts. First the deflection was to be measured for calculation of MOE, see Figure 6.6. The second part of the test was to load the beam until rupture, see Figure 6.7. The clamps were attached to the beam and the roller bearings were checked to be in the right place, so the span would be correct and the load points in position. The Linear Velocity ~ Displacement Transducer (LVDT) was positioned under the beam in the middle of the span for measurement of the deflection. The beam was then loaded to about 2.5 kN, at the best of our ability according to the load rate of 9 kN in 5



Four point bending test

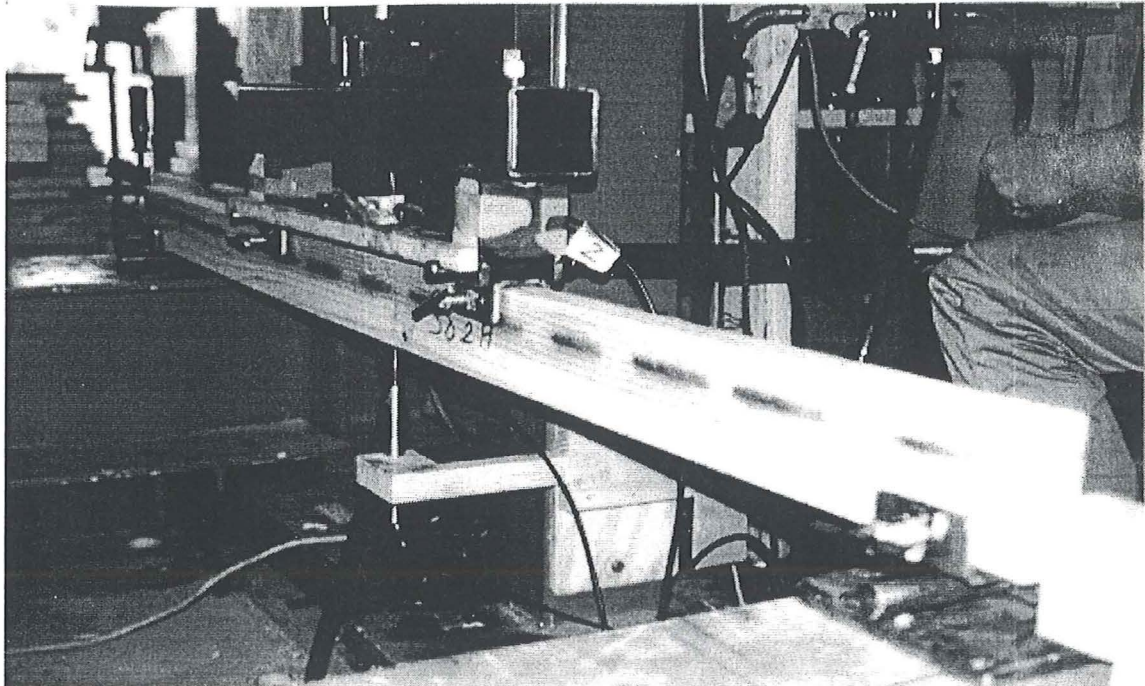


Figure 6.6
First part of the Four point bending test, measurement of deflection for calculation of MOE. The LVDT is positioned in the middle of the span.

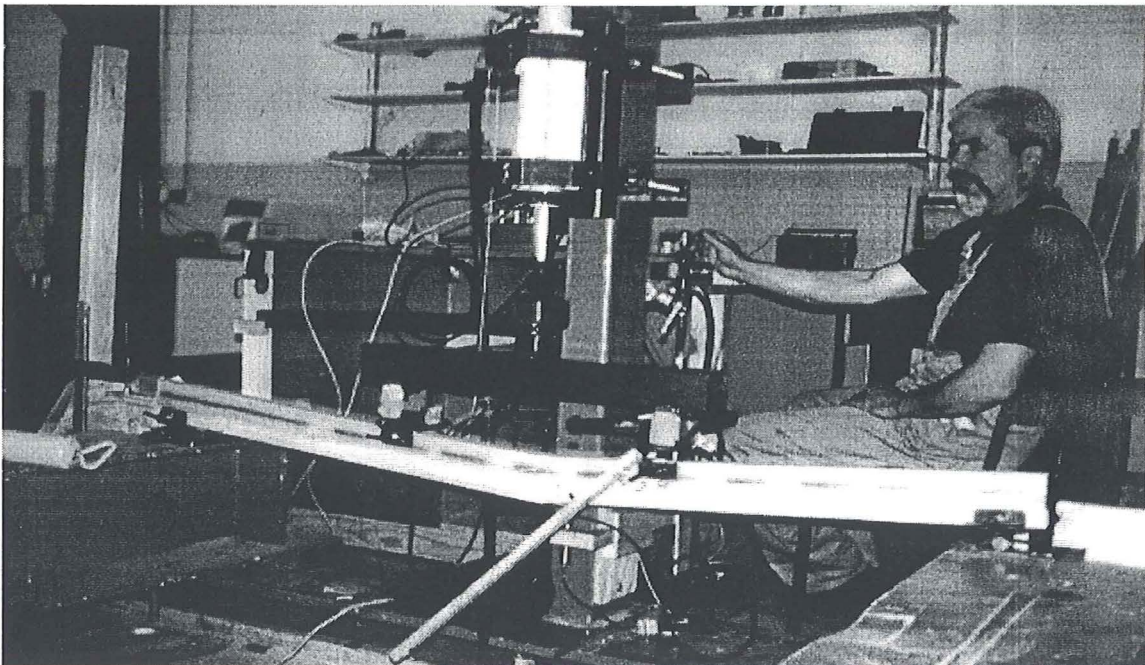


Figure 6.7
Second part of the Four point bending test. The beam is loaded until rupture by Mr Honeychurch



Four point bending test



minutes. After that the beam was unloaded. The same stick was then reloaded, at the stipulated load rate, until rupture. The LVDT stayed in its place until about 4 kN. This turned out to be very fortunate, see 7.5 Saving the data.

6.4 Problems and solutions

As mentioned in The setup two sensors were attached to the beam for the first ten tests. When the beam broke and splintered substantial damage was caused to the sensors. Comparing the signals from AE1 on the beam and AE2 on the steel bar revealed that AE2 was just as good to use for our purposes, see Appendix B. The solution was to rely on AE2. An advantage with this was that time could be saved, as the clamp with the sensors did not have to be attached every time.

A disadvantage with the location was that the room was shared with the workshop of the Department of Architecture. The sensors are very sensitive indeed and all sound is likely to be picked up by the sensors. This problem became obvious when students started doing metal work and welding. The AE went rocket high. We got them to stop so the test could be finished. Afterwards we ran some trials to see what kind of sound that affected the sensors and what we could do about it. As mentioned metal work and welding had a great impact. Hammering or clapping ones hands at a distance of about 5 m was clearly detected. Students doing timber work in the other end of the room and even cars passing by outside was detectable, but the difference was very small. Fortunately normal conversation was not noticeable. We managed to solve the worst parts. The students were able to do most of their metal work when we did not perform any tests and some of it could be done in between tests. No work was to be done in the part of the room where the test was carried out. The rest of the noise did not have that much influence on the AE, and as we could not have the entire room for ourselves we just had to live with it.

The often dramatic failure of the beams caused the sensors to slowly move out of their location. We did not want to add more pressure to the top of the sensors' case, as this actually could destroy the case. Instead foam was put around the sensors and secured with tape to obstruct the movement of the sensors. In addition it was regularly checked that the sensors were in place and that the screw and the wedges exerted sufficient pressure.

When checking previous data I found that there was no difference between the AE at the load step and the maximum AE for the interval. The program also failed to register the load at rupture. This did not have very much influence on the calculation of Modulus of Rupture (MOR) as the load step was only 0.20 kN. The maximum load had to be anticipated to be the one at the last registered load step. The greatest fault this assumption can give when it comes to MOR is +1.14 MPa or about 2%. As the AE is considered to be highly dependent on the load rate the use of maximum AE is probably better for evaluation than the AE at the load step. Unfortunately the problem was discovered when almost all of the Scottsdale samples were broken. It was Mr Nolan who finally found the



Four point bending test



error, one loop to much. After correcting this we did eight samples and checked again. There was still something wrong. It turned out to be an indexing of an array that had been disabled. At last I managed to get the program right. A description of the final version called Beam test 2-3.vi is found in Appendix A.

When one of the rollers fell into the pit under the floor Mr Honeychurch saw that the pump was leaking oil. He was able to fix the leak and with some new oil the test could continue.

As mentioned above the AE was assumed to go hand in hand with the load rate. When the load was increased at a higher rate there seemed to be a direct correspondence in the AE. Even if we did our best to increase the load at the same pace it is very easy to go a bit ahead or fall somewhat behind. There was not much we could do about it, as we only had access to a manual jack. When doing experiments like this in the future I will recommend that if possible an automatic jack is used. That way the load rate will be the same all the time and the question will not arise. I think the conclusion of this chapter is that, if possible, you should always do an experiment twice.

6.5 Saving the data

When starting the VI Beam test 2-3.vi the program automatically asked for a name for the file to save. The name was chosen as the number of the stick and an "A" indicating Four point bending test. For the first part of the test, when deflection was measured, the number 1 was added and the second part of the test was indicated by number 2. For instance T177A-2 is the second test in Four point bending of stick 177 from Tarpeena.

"Dummy" became a quite usual word during the test, referring to trials that had to be restarted. For some reason the LVDT very often gave maximum reading from the beginning. After starting all over again it almost always behaved itself, else yet another restart would do the trick. We did not find any reason for this to happen. As mentioned above the program needed a name for the test before it could be executed. This was very good as no test could be forgotten to be saved. What took us long time to notice though was that the program would not overwrite an existing file, even though it asked if we wanted a file overwritten. The consequence of this was that when we chose the same file name after a dummy the new test was not saved. Instead we ended up with a lot of dummies. This was no catastrophe though. The deflection could be evaluated from the second test instead of the first. From the second test six of them were lost due to dummies.

In Appendix C is a table of how the data is presented and explanations of what the numbers stand for.



Analysis of the test



7. Analysis of the test

7.1 Rejection of samples

One should always be very conservative when it comes to rejection of samples. The reason for disregarding a test must have a good grounding. I have found two purposes for the rejection of samples. The first one is that the test is a “dummy”, as discussed in 6.5 Saving the data. There is just no data from the test to evaluate. The second cause is that the AE did not work properly. For S90A-2 it had to do with the fact that the AE was just not turned on and hence no AE was recorded. The other samples rejected because of AE failure was due to software problem with indexing, as mentioned in 6.4 Problems and solutions. For these the AE are the same for all readings, which certainly is not true. The samples and their reason for rejection are shown in Table 7.1. From Scottsdale a total of 6 samples were rejected leaving 64 to evaluate. The equivalent for Tarpeena was 9 samples rejected leaving 91 for evaluation. Apart from this I have found no legitimate reason for not treating a test as a successful one. All analysis is based on the successful tests only. In Appendix D is the data used in the analysis.

Sample	Rejected		Sample	Rejected		Sample	Rejected
S90A-2	AE failure		S91A-2	Dummy		T155A-2	AE failure
S132A-2	Dummy		T179A-2	Dummy		T156A-2	AE failure
S131A-2	Dummy		T173A-2	AE failure		T165A-2	AE failure
S106A-2	Dummy		T159A-2	AE failure		T150A-2	AE failure
S74A-2	Dummy		T128A-2	AE failure		T170A-2	AE failure

Table 7.1
The rejected samples and the reason for doing so.

7.2 Sample distributions

The Central Limit Theorem states that, without exception, “regardless of the shape of the distribution of the individual values within a population, sample averages selected from a population will be approximately normally distributed” (15). If the selection of the samples was random and there are enough samples the distribution is expected to be approximately normal. The histograms with its fitted normal mass distribution are visualised in Figure 7.1 for Scottsdale and in Figure 7.2 for Tarpeena. The data for the histograms and normal mass distribution is found in Appendix D.



Analysis of the test

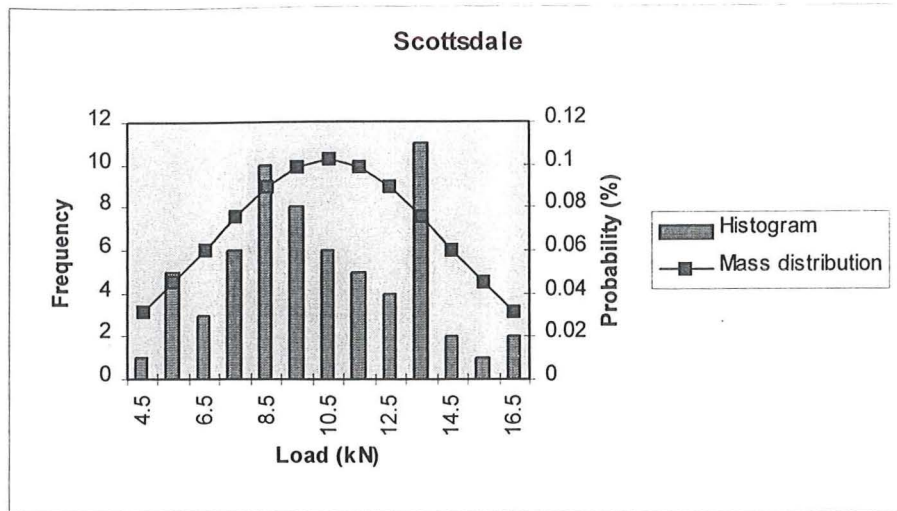


Figure 7.1
Histogram and fitted normal mass distribution for the samples from Scottsdale.

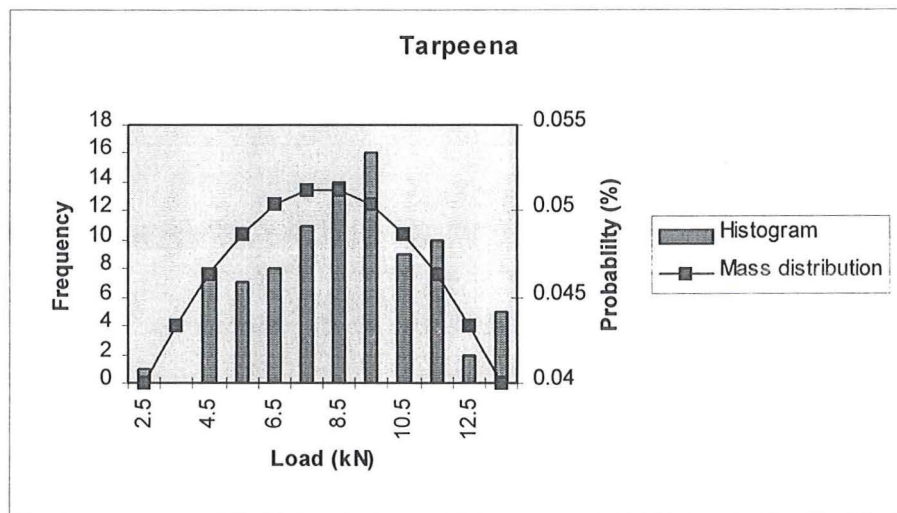


Figure 7.2
Histogram and fitted normal mass distribution for the samples from Tarpeena.

For a better evaluation of the histograms we are going to use the following equations and the mode, which is the value that occurs most frequently (16).

$$\text{Arithmetic mean } X_m = \frac{\sum_{i=1}^n x_i}{n} \tag{Equation 7.1}$$



Analysis of the test



where x_i is the i th value of variable X ($i = 1, 2, \dots, n$)
 n is the number of values

$$\text{Estimated population standard deviation } S_x = \sqrt{\frac{\sum_1^n (x_i - X_m)^2}{(n-1)}}$$

Equation 7.2

where x_i is the i th value of variable X ($i = 1, 2, \dots, n$)
 X_m is the arithmetic mean, Equation 7.1
 n is the number of values

The Scottsdale distribution looks fairly normal except for a second peak at 13 kN. This raises the question of bias. I think it has more to do with how the Tasmanian timber grows than failure to randomly select the samples. As discussed in 5.4 Scottsdale and Tarpeena the radiata used at Scottsdale is cut at about an age of 30 years. The size of the log is highly dependent on the growing conditions. The logs taken from high altitude have much less diameter than others at the same age. These slow growing trees are likely to be stronger than the faster growing ones. A change in the sawing pattern causing a mix between logs of small and large diameter and hence a difference in strength is what I assume is behind the “twin peak” distribution from Scottsdale. If so the pattern of the histogram shows how much the properties for radiata at Scottsdale can vary, and it is a good picture of the radiata population for the sawmill. It is not possible to trace an individual stick from which kind of log it came from or from what area it was cut. Therefore my theory is more of a hunch, as it can not be tested. Another factor is the sample size. With such an inhomogenous material as radiata pine, 64 samples might be too few to achieve an approximately normal distribution.

Some basic statistics for Scottsdale,

$$X_m = X_m = \frac{657.16}{64} = 10.27 \text{ kN} \tag{Equation 7.1}$$

$$S_x = \sqrt{\frac{561.18}{(64-1)}} = 2.98 \text{ kN} \tag{Equation 7.2}$$

mode = 13 kN

The mean is between the two peaks, but does not correspond very well with the mode. For the mathematical normal distribution approximately 68 % of the area will fall between -1σ and $+1\sigma$ from the mean. Another $\pm\sigma$ will add about 28 % to the area. For



Analysis of the test



any value of X_m , σ or n this will be the case for any normal distribution (16). In spite of the low correspondence with the normal distribution because of the two peaks the percentage for -1σ to $+1\sigma$ is 66 % of the total area and an extra $\pm 1\sigma$ adds another 36 %. This is quite close to the normal distribution.

The correspondence with the normal distribution looks much better for Tarpeena. This is hardly surprising as the radiata come from plantations, which probably gives a more homogenous material, and that the sample size is larger.

The basic statistics for Tarpeena are,

$$X_m = \frac{785.91}{91} = 8.64 \text{ kN} \quad (\text{Equation 7.1})$$

$$S_x = \sqrt{\frac{564.57}{(91-1)}} = 2.50 \text{ kN} \quad (\text{Equation 7.2})$$

$$\text{mode} = 9 \text{ kN}$$

The mode and the mean are very close. The same comparison as for Scottsdale yields 67% of the total area at $\pm 1\sigma$ and an additional 19% for an extra -1σ respective 14% for an extra $+1\sigma$. This is also close to the limits of the normal distribution.

My conclusion is that neither Scottsdale or Tarpeena can be assignable to be bias, but it must be said that Tarpeena has more certainty. Considering all the data and the time available it is therefore better to look closer into the Tarpeena results.

7.3 AE2 Max analysis for Tarpeena

The AE is thought to be very sensitive to the load rate. Previous research at the University of Tasmania regarding AE and hardwood indicated that the AE dropped off within seconds after the load being applied (17). This problem may partly been reduced with small load steps of 0.20 kN. A further reduction is assumed by the use of the maximum AE for the interval, which I therefore have chosen to look more into. In Appendix D is the data used for the AE2 Max analysis. Microsoft Excel was used for the analysis. The term "cell" means the cell in an Excel worksheet.

7.3.1 First support for the theory

The first step was to gather all AE information to see if there was some kind of trend. The number of readings ranged from 14 readings for the weakest to 83 readings for the strongest stick. The AE values had to be transformed into one representative stick with a



Analysis of the test



suitable, 40 eg, number of readings. To do this the AE data for each stick was compressed or extended to 40 readings. The procedure is shown in Figure 7.3.

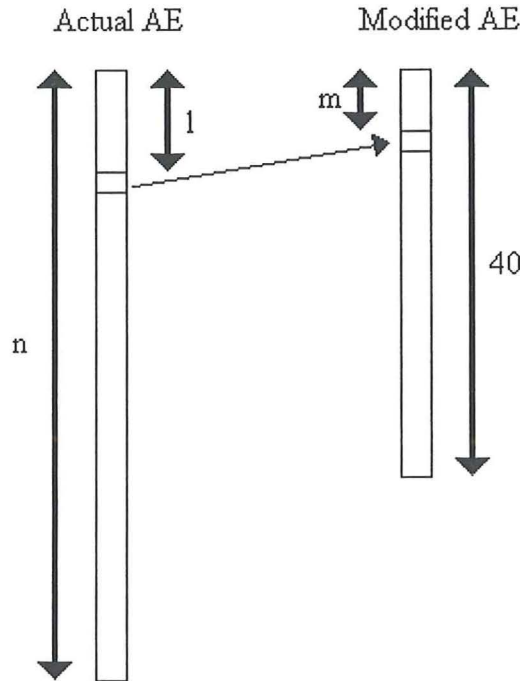


Figure 7.3
The principal for turning the actual AE of a stick with n readings into the modified one with 40 readings. The value for element m of the modified stick is calculated from element l of the actual stick.

To give a further explanation of the procedure I will use the data for T177A-2 in Appendix C and the notation from Figure 7.3. Number of values (readings) $n = 28$. If we for instance wanted the value for the 18th cell of the modified stick the corresponding cell l of the actual stick is calculated with the following equation.

$$\text{Cell of actual stick } l = \frac{m \times n}{40} \tag{Equation 7.3}$$

where m is the cell of the modified stick
 n is the number of values

For T177A-2 the corresponding cell l to the 18th cell of the modified stick is,

$$l = \frac{18 \times 28}{40} = 12.6 \tag{Equation 7.3}$$



Analysis of the test



The cell numbers are all integer so a simple linear extrapolation between cell 12 and cell 13 is used. The value for cell m is given by Equation 7.4.

$$AE(m) = AE(trunc(l)) + (AE(trunc(l+1)) - AE(trunc(l))) \times (l - trunc(l))$$

Equation 7.4

where AE () is the value of the cell number within the brackets
trunc () is truncation of the value within the brackets
l is the cell of actual stick, Equation 7.3

For T177A-2 in this little example this would be,

$$AE(18) = AE(12) + (AE(13) - AE(12)) \times (12.6 - 12) =$$

(Equation 7.4)

$$= 0.08301 + (0.12207 - 0.08301) \times 0.6 = 0.10645 \text{ V}$$

The sum for the same reading of every one of these modified sticks was divided by the number of sticks to get the AE for that reading for the representative stick. In Figure 7.4 is the diagram for the representative stick. The reason for the high noise for the first readings has to do with the application and settling of the load. The theory I worked after, based on knowledge from a similar test on hardwood, was that a change was expected at about 80% of maximum load. The pattern of Figure 7.4 definitely supports the theory. Just over reading 30 a change takes place. The ratio between volt and reading increases from about 0.012 to about 0.044. For the representative stick a voltage of 0.5V to 0.6V is in the beginning of this change, corresponding to 77.5% to 82.5% of maximum load.

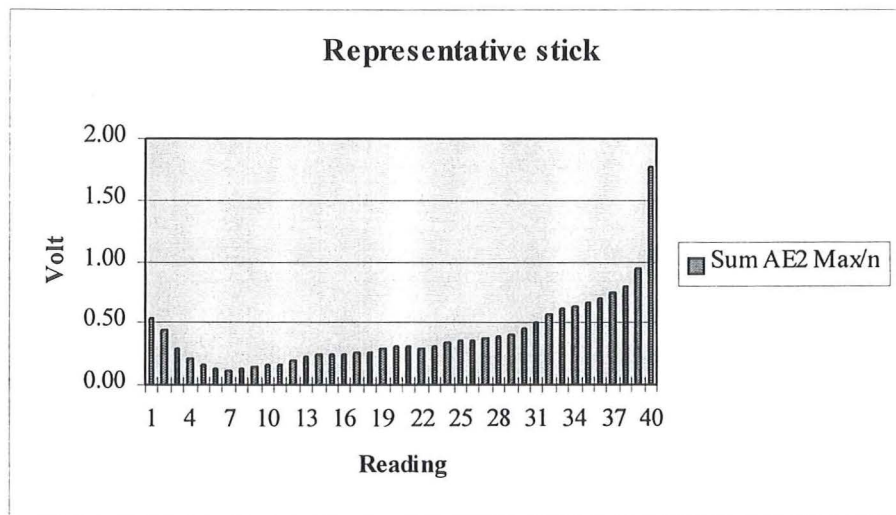


Figure 7.4
The diagram for the representative stick, derived from the sum of all modified sticks and divided by the number of sticks. A change in the ratio volt / reading takes place around reading 30.



Analysis of the test



7.3.2 Different patterns

The next thing to do was to look at each individual test. The first support for the theory indicated a significant increase in the ratio between volt and reading at around 80% of maximum load. The AE when this change in the ratio took place would be 0.5 V to 0.6 V. This formed the input for the following analysis. AE2 Max, the load rate and the aimed load rate were plotted against the reading for all sticks. A slope less than the aimed load rate means a higher load rate than the aimed 9 kN in 5 minutes. The relation between AE and load rate is not at all obvious, which is unexpected. A nearly constant load rate can show an increase or decrease in AE, and a high load rate is quite often not followed by high AE and vice versa. Very often the load rate was actually managed to be kept at the aimed pace, but diversions from this did not have the impact we thought it would have. The AE can be divided into three different patterns. These are called Type I, Type II and Type III. Representative samples of these are shown in Figure 7.5, Figure 7.6 and Figure 7.7 respectively. All types have the initial noise from the settling of the load. Therefore the first 10 readings have not been taken into account. Apart from that they are different in their appearance.

What distinguish Type I is that the AE2 Max does not reach 0.6 V until 90% or more of the maximum load. This means that the warning comes very late and that the stick by then is likely to have been damaged. 23% of the samples can be assigned to this group. In fact 15% of the samples did not give any warning at all at the 0.6 V level before rupture. A remarkable high wastage.

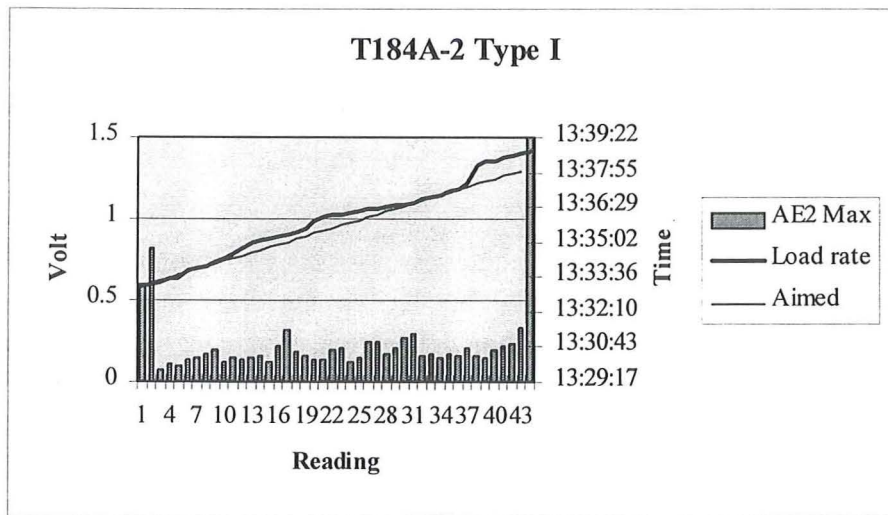


Figure 7.5
T184A-2 as a characteristic for a pattern of Type I. AE2 Max does not reach up to 0.6V before 90% of maximum load.



Analysis of the test



Type II is characterised by the AE2 Max reaching 0.6 V somewhere between 50% and 90% of maximum load. If using AE for stress grading the indication to unload the beam would come in a safe range of the beam's capacity for this type. The majority of the samples, 60%, can be classified as Type II.

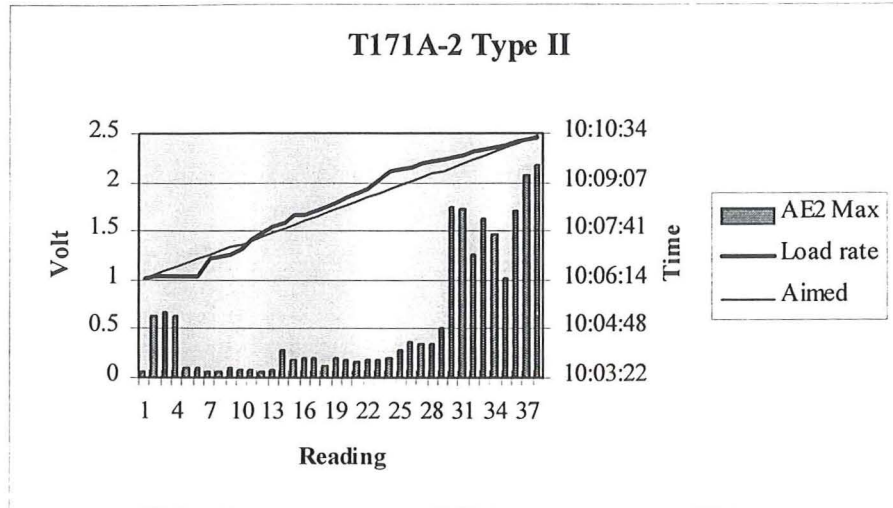


Figure 7.6
Type II is represented by T171A-2. AE2 Max reaches 0.6V somewhere between 50% and 90% of maximum load.

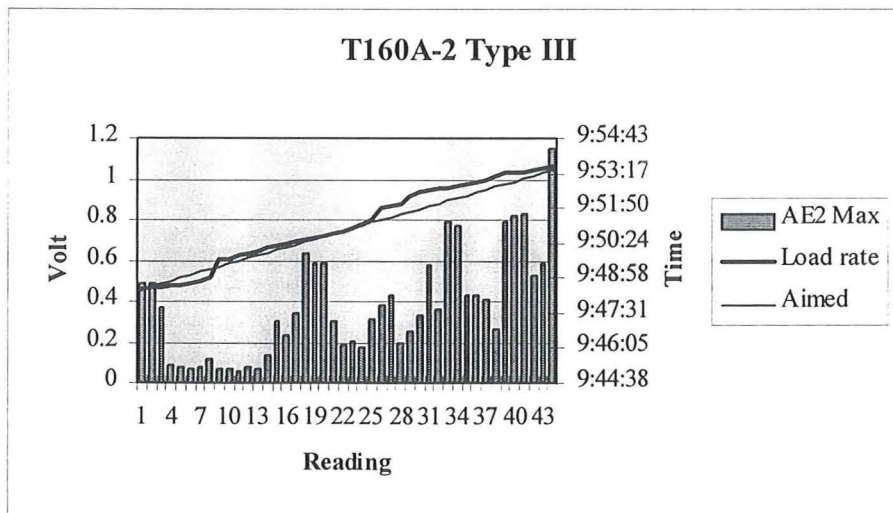


Figure 7.7
Sample T160A-2 as an illustrative for Type III. Here the noise is high and frequent throughout. AE2 Max reaches 0.6 V earlier than 50% of the maximum load.



Analysis of the test



The third type, Type III, has high and frequent noise at an early stage. AE2 Max will get up to 0.6 V before 50% of the maximum load. That means that the stick is assumed to have less than half of its real capacity. 17% of the samples are to be assigned to Type III.

The reading when AE2 Max exceeds 0.6 V versus ultimate reading is plotted in Figure 7.8. Type I-III use different percentage of the ultimate capacity. Up to 50%, 50-90%

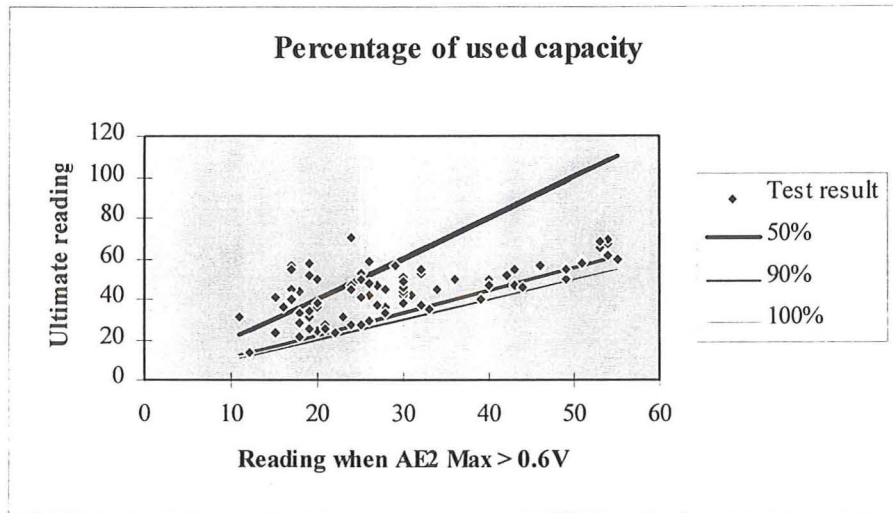


Figure 7.8
The percentage of used capacity at AE2 Max > 0.6 V. The 14 sticks, 15%, that failed before AE2 Max reached 0.6 V are not represented. Lines corresponding to the limits of Type I-III, give the level of security or waste of capacity for each data point.

respective 90-100%. Lines corresponding to these limits are also plotted in Figure 7.8. The distance in the y-direction gives the level of security or wasted capacity of each stick. Note that there are only 77 data points. The 14 sticks, 15%, which failed without warning are not represented in the diagram.

I have not found any cause to be able to tell in advance what kind of pattern a single stick will give. All kinds of sticks have ended up in all three types of patterns. It does not seem to have anything to do with if the stick is fairly free from knots or have a lot of them. Neither is there any relation between different modes of failure and a special type. I think it is as usual when it comes to radiata that these differences are subject to the vast variation in the material itself.

7.3.3 Statistics of the analysis

The theory that is to be proved is called the null hypothesis, H_0 . An alternative hypothesis, H_1 , is needed in case the indication is that H_0 is false. H_1 must be inconsistent with H_0 . It is not necessary that H_0 is stated as an equality, but it is strongly



Analysis of the test



recommended, as that makes later analysis easier. If H_1 is chosen as a nondirectional inequality it signifies a two-tailed test of the hypothesis (15).

When testing a hypothesis we are confronted with two types of errors. If we reject H_0 when it is true we have made an error I. Acceptance of H_0 when it is false will give an error II. Two kinds of correct decisions can also be made. This is represented in Table 7.2 (18). One type of error can not be decreased without increasing the other one. In research we do not want to reject H_0 when it is true, making an error I. On the other hand is it not good to accept all H_0 as true, and thereby eliminating error I. The level of significance, α , is the probability that H_0 is true and that the result arose by random error (18). An α of 0.01 will only have 1% chance that random error is the reason for differences. At an α of 0.05 the probability of random error has increased to 5%. Hence a higher α is a stronger criteria that H_0 actually is true. The level of confidence, $1-\alpha$, is how confident we are to reject H_0 when it is false, thereby making a correct decision. If H_0 can not be rejected at the chosen confidence level it is actually accepted as being true.

Decision	Accept H_0	Reject H_0
Truth		
H_0	Correct	Error I
not H_0	Error II	Correct

Table 7.2
The possible decisions when testing a hypothesis. An error I will reject a true hypothesis, while an error II will accept a false one. Two correct decisions can also be made.

A relation between stress and AE was established in Figure 7.4, with the so called representative stick. The wide variety of patterns for the AE of the single tests was though not as encouraging. From the diagram of each test the first reading when AE2 Max reached 0.6 V and the ultimate reading for that test was registered. According to the result from the representative stick the reading at 0.6 V times 1.212 would yield the ultimate reading. If the reading when AE2 Max exceeds 0.6 V versus ultimate reading, as plotted in Figure 7.8 above, was consistent with the theory all data point would lie on a line with a slope of 1.212. This was of course not the case.

Linear regression fits a line through a set of observations by using the least squares method. In this case it is obvious that the regression line should pass through the origin of coordinates. The formula for calculating the slope of the regression line, b , through the origin of coordinates is (19),



Analysis of the test



$$\text{Slope of regression line } b = \frac{\sum_1^n (x_i \times y_i)}{\sum_1^n (x_i)^2} \tag{Equation 7.5}$$

where x_i is the i th value of variable X ($i = 1, 2, \dots, n$)
 y_i is the i th value of variable Y ($i = 1, 2, \dots, n$)
 n is the number of values

$$b = \frac{107840}{77891} = 1.384 \tag{Equation 7.5}$$

The data is plotted in Figure 7.9 together with the regression line, slope $b = 1.384$ and the theoretical slope $\beta = 1.212$.

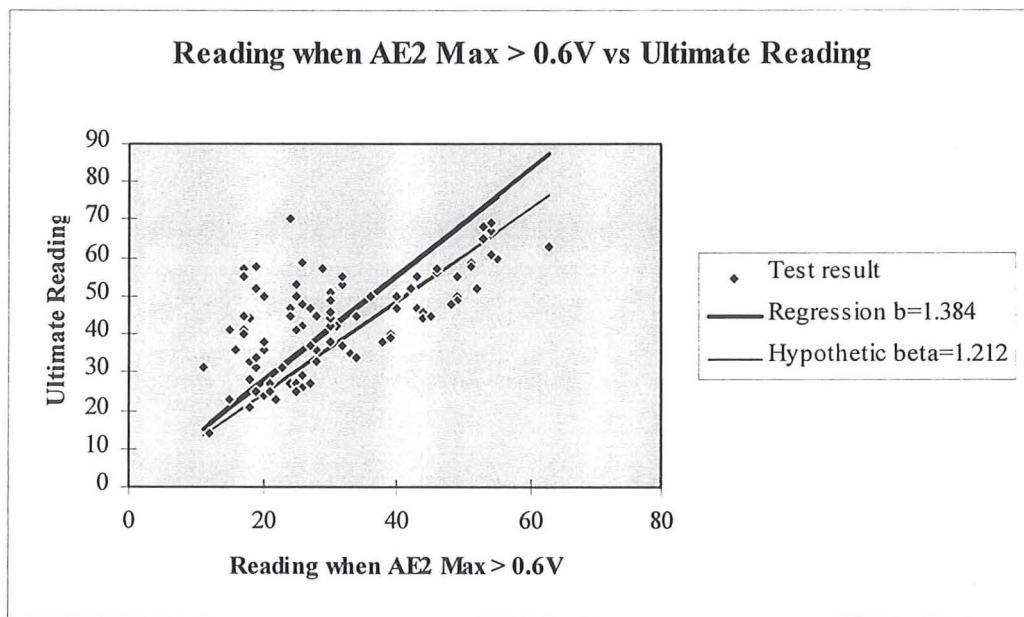


Figure 7.9
 The regression line, slope $b = 1.384$, achieved with the least square method for the data and the hypothetical slope $\beta = 1.212$.

We need a suitable statistic to test if the difference between the slopes arose by random error or not. If the whole population had been tested the parameters for the population could have been calculated and the normal distribution would be the appropriate to use. As this analysis is based on the results from a small number of samples compared to the population only estimations of the parameters can be obtained. The Student's t



Analysis of the test



distribution takes this into consideration. Therefore the Student's t test is chosen as the suitable test. Additional equations required for the test are (19),

The regression line $y'_i = b \times x_i$ Equation 7.6

where b is the slope of the regression line, Equation 7.5
 x_i is the i th value of variable X ($i = 1, 2, \dots, n$)
 n is the number of values

$$\text{Student's } t = (b - \beta) \times \sqrt{\frac{(n-2) \times \sum_1^n (x_i - X_m)^2}{\sum_1^n (y_i - y'_i)^2}}$$
 Equation 7.7

where b is the slope of the regression line, Equation 7.5
 β is the theoretical slope
 n is the number of values
 x_i is the i th value of variable X ($i = 1, 2, \dots, n$)
 X_m is the arithmetic mean, Equation 7.1
 y_i is the i th value of variable Y ($i = 1, 2, \dots, n$)
 y'_i is the regression line, Equation 7.6
 $(n-2)$ is the degrees of freedom

The hypothesis to be tested are,

H_0 : the slope of the regression line = 1.212

H_1 : the slope of the regression line \neq 1.212

$$t = (1.384 - 1.212) \times \sqrt{\frac{(77-2) \times 10911}{13385}} = 1.345$$
 (Equation 7.7)

As H_1 is stated as a nondirectional inequality a two-tailed test should be used. If the value of the test statistic 1.345 is less than the tabulated value there is not sufficient evidence to reject H_0 (15). Interpolation for 75 degrees of freedom at a significance level of 0.05 in a table with critical values of t yields 1.995, hence H_0 can not be rejected at a confidence level of 95%. The equivalent critical value at a significance level of 0.10 is 1.668, consequently H_0 can not even be rejected at a confidence level of 90%. The probability is thus more than 10% that the difference in slopes arose from random error, which is more than acceptable.



Analysis of the test



7.3.4 Comparison between AE2 Max and MOE to predict strength

Deflection and load are measured in mechanical stress grading for calculation of MOE. MOE is then used to predict the strength as MOR. Data for MOE and MOR is found in Appendix D

AE2 Max versus Ultimate reading and MOE versus MOR were compared to see how good they are to predict strength. The units Ultimate reading and MOR are basically the same. They are both a constant times the load at rupture, therefore the comparison of the correlation is relevant even though the load is expressed in different units. Correlation is a measure of the relationship between two variables. As we want the correlation between linearly related variables the Pearson product moment correlation coefficient r is used. The equation for r is (16),

$$\text{Correlation } r = \frac{\sum_1^n (x_i \times y_i) - \frac{\sum_1^n x_i \times \sum_1^n y_i}{n}}{\sqrt{\left(\left(\sum_1^n (x_i)^2 - \frac{\left(\sum_1^n x_i \right)^2}{n} \right) \times \left(\sum_1^n (y_i)^2 - \frac{\left(\sum_1^n y_i \right)^2}{n} \right) \right)}} \quad \text{Equation 7.8}$$

where x_i is the i th value of variable X ($i = 1, 2, \dots, n$)
 y_i is the i th value of variable Y ($i = 1, 2, \dots, n$)
 n is the number of values

The correlation between MOE, variable X, and MOR, variable Y is,

$$r = \frac{47085060.6 - \frac{930646 \times 3855.5}{77}}{\sqrt{\left(\left(11440038120 - \frac{866101977316}{77} \right) \times \left(208949.5 - \frac{14864770.1}{77} \right) \right)}} = 0.278$$

(Equation 7.8)

For reading when AE2 Max > 0.6 V, variable X, versus ultimate load, variable Y, the correlation is,



Analysis of the test



$$r = \frac{107840 - \frac{2271 \times 3405}{77}}{\sqrt{\left(\left(77891 - \frac{5157441}{77}\right) \times \left(162689 - \frac{11594025}{77}\right)\right)}} = 0.645 \quad \text{(Equation 7.8)}$$

The correlation is much better for AE2 Max than for MOE when it comes to predict strength, see Figure 7.10 and Figure 7.11. Hence AE is a more reliable way to stress grade timber.

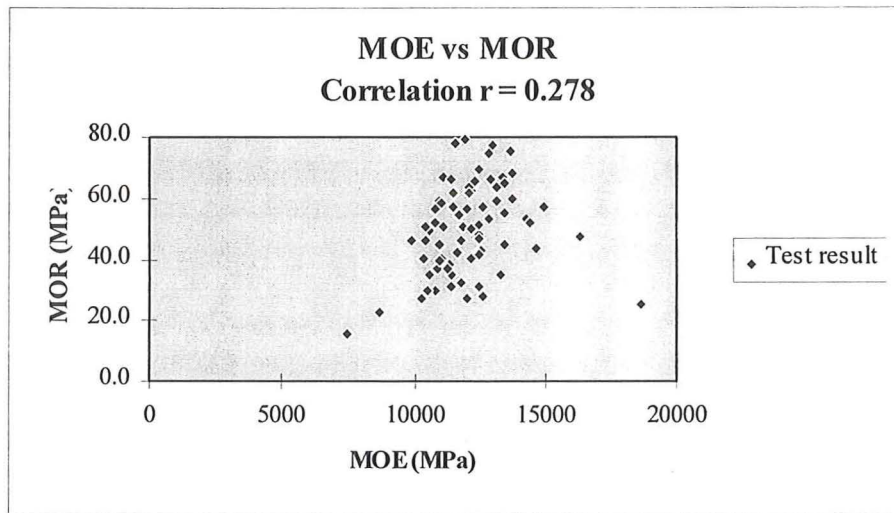


Figure 7.10
MOE versus MOR for the test. The correlation is 0.278.

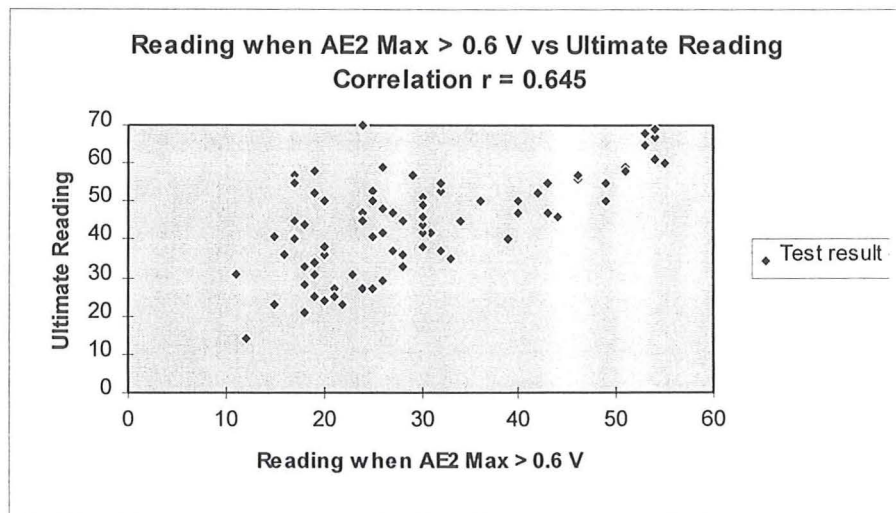


Figure 7.11
For AE versus Ultimate reading the correlation $r = 0.645$.



Conclusions



8. Conclusions

The summation of AE2 Max for all sticks into a representative stick revealed an increased rate of AE2 Max at around 80% of maximum load. The change corresponds to an AE2 Max of 0.5-0.6 V.

From the division of AE-pattern into Type I-III it was concluded that 23% did not give any warning before 90% of maximum load. In fact 15% actually ruptured before AE2 Max reached 0.6 V. For the majority of 60% the 0.6 V level was reached at 50-90% of maximum load. The remaining 17% gave their AE warning at less than 50% of maximum load.

For the representative stick the reading at 0.6 V times 1.212 gave maximum load. The slope of the regression line for the samples was 1.384. The hypothesis that there was no difference between the regression line and the theoretical slope could not be rejected at a confidence level of 90%, which is more than acceptable.

The correlation for the use of AE to predict ultimate load was 0.645. For MOE to predict MOR the correlation was only 0.278. AE is therefore a more reliable way to stress grade radiata. The high wastage though when using AE has to be considered. At this stage there will be beams that actually break during the grading with AE. This is not the case when MOE is used to grade timber. The problem with MOE though is that, because of the low correlation, more beams will be graded too high or too low. The ones graded too high constitute a risk in construction as they will actually break at a lower load than expected. For the beams graded too low there is only a loss of used strength.

AE has proven to be a good way to stress grade radiata pine. Further research will certainly be able to lower the wastage to an acceptable level and make the method applicable to the industry. For this the speed of the method must also be improved and the problem with noise interfering with the AE must be solved.



Appendix A



Beam test 2-3.vi

The VI used for this research is called Beam test 2-3.vi. It was modified by me from Beam test 2-2.vi following the instructions from Research Officer Gregory Nolan, at the Department of Architecture at the University of Tasmania, who created Beam test 2-2.vi.

Panel window

In the Panel window, also called Front panel, there are a lot of indicators, buttons and scales. The Panel window is shown in Figure A1. The lower part of the Front panel consists of controls. These are the LVDT Initial Controls, Channel Controls, Load interval control and Diagnostic controls. The Load interval control determines when the program should take a reading. The program takes a reading at each load step, detects the maximum AE between load steps and the final load at rupture. The controls are to be set by the operator and provide the input to the Diagram window, also called Block diagram. In the top right corner is an Off-button. By pressing this the execution of the program will stop. Thereby the Off-button is also an input to the Block diagram. The rest of the Front panel contains indicators. The indicators will show the output from the Block diagram. Each digital control has its own digital indicator. In this way you will see the results as a gauge as well as with its numeric value. The VI will also plot PSI versus deflection in the graph.

Diagram Window

The Diagram window is the actual program in the graphical program language “G”. The Diagram window of Beam test 2-3.vi has three frames, numbered 0, 1 and 2. This so called Sequence structure is the LabVIEW way of controlling the order in which the nodes are executed. Text based program languages are executed in the order they appear, while in data flow programming a node is executed when the necessary data is available at all the node inputs (20). LabVIEW start to execute the diagram inside frame number 0, then number 1 and so on.

Here follows a brief description of how Beam test 2-3 works. The program’s frames 0, 1 and 2 are found in Figure A2, A3 and A4 respectively. The symbols described are marked with the corresponding number in the frame where it appears. Number 0 is found in Figure A2, while number 1 to 17 are found in Figure A3.



Appendix A



0



This returns the voltage from the instrument measuring deflection and sends the information to 8.

1



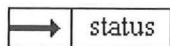
The instruments used in the test convert their respective measured values into a voltage, which is sent to the DAQ. The Config symbol collects its input from the DAQ through the Device, Channels and the Buffer size in scans. These are set by the operator on the Front panel of the VI. The Start symbol gets the information about Buffers to acquire from the Front panel. All the data is passed on to the Read symbol, where it is made in to an array. The array has one row with elements. If an error appears it is sent on to 2 and 3.

2



These register errors and if an error occurs an error message will show on the Front panel.

3



If an error occurs the execution of the program will stop.

4

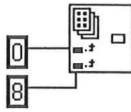
This wire between 1 and 5 indicates that it is in form of an array. The array has one row with elements. Each element is a numeric value of the voltage acquired in 1.



Appendix A

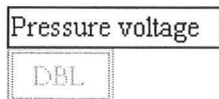


5



This symbol, the index array, accesses an element in an array. The first row in the array is number zero, the second number one etc. In this case there is only one row in the array. We identify this row by connecting it to the zero next to the symbol. In the second box connected to the index array symbol we print the number of the element in the array we want to access. The elements are numbered in the same way as the rows in the array. The first element is number zero, the second number one etc. In this case there is an eight in the box, which will give us the value in element number nine.

6



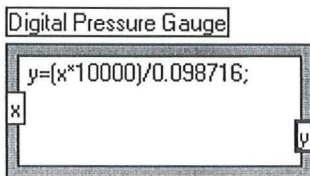
This will present the numeric value of the element chosen in 5 on the Front panel. On the Front panel you will see it in form of a digital indicator. The same procedure is valid for the Interface LC and the Centre LVDT-25R.

7



In the same way as in 6 this will display a numeric value on the Front panel. You will see it in a vertical indicator as well as in its digital display. It works in the same way for AE2 and AE3.

8



X is given the numeric value of the voltage from 5. By the equation in the box LabView will calculate a y-value. By calibration and measurements of the instruments used in this experiment you get the equation to turn the voltage into



Appendix A



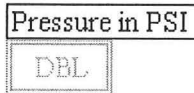
another desired unit. In this case we will get the y-value as pressure in PSI. By altering the equation we get the Load Centre (kN) and Displacement-Centre.

9



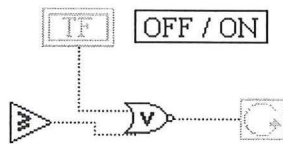
The max and min function compares the current value with the highest so far and replaces it if the current value is higher. This will give us the maximum load respectively the maximum AE in the interval.

10



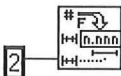
The calculated y-value from 8 is send on to this symbol. It will show the result on the Front panel as a horizontal indicator with a digital display.

11



Without any errors the program will run until the operator pushes the OFF-button on the Front panel or until the Load centre is higher than the previous load plus the load interval.

12



This converts the numeric value to a floating-point formatted string. The number in the box will give the precision for the string. For instance the numeric value 1.2 would be converted to the string as 1.20 in this case.



Appendix A



13



With this the system is able to get the date and time for every measurement.

14



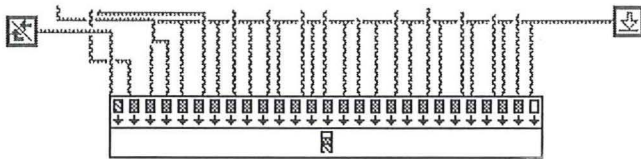
By bundling we can get the Displacement-Centre and Load Centre in the same diagram.

15



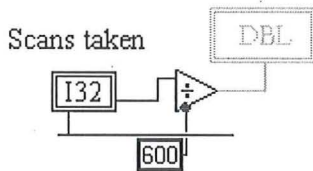
Returns the number of elements in the input array.

16



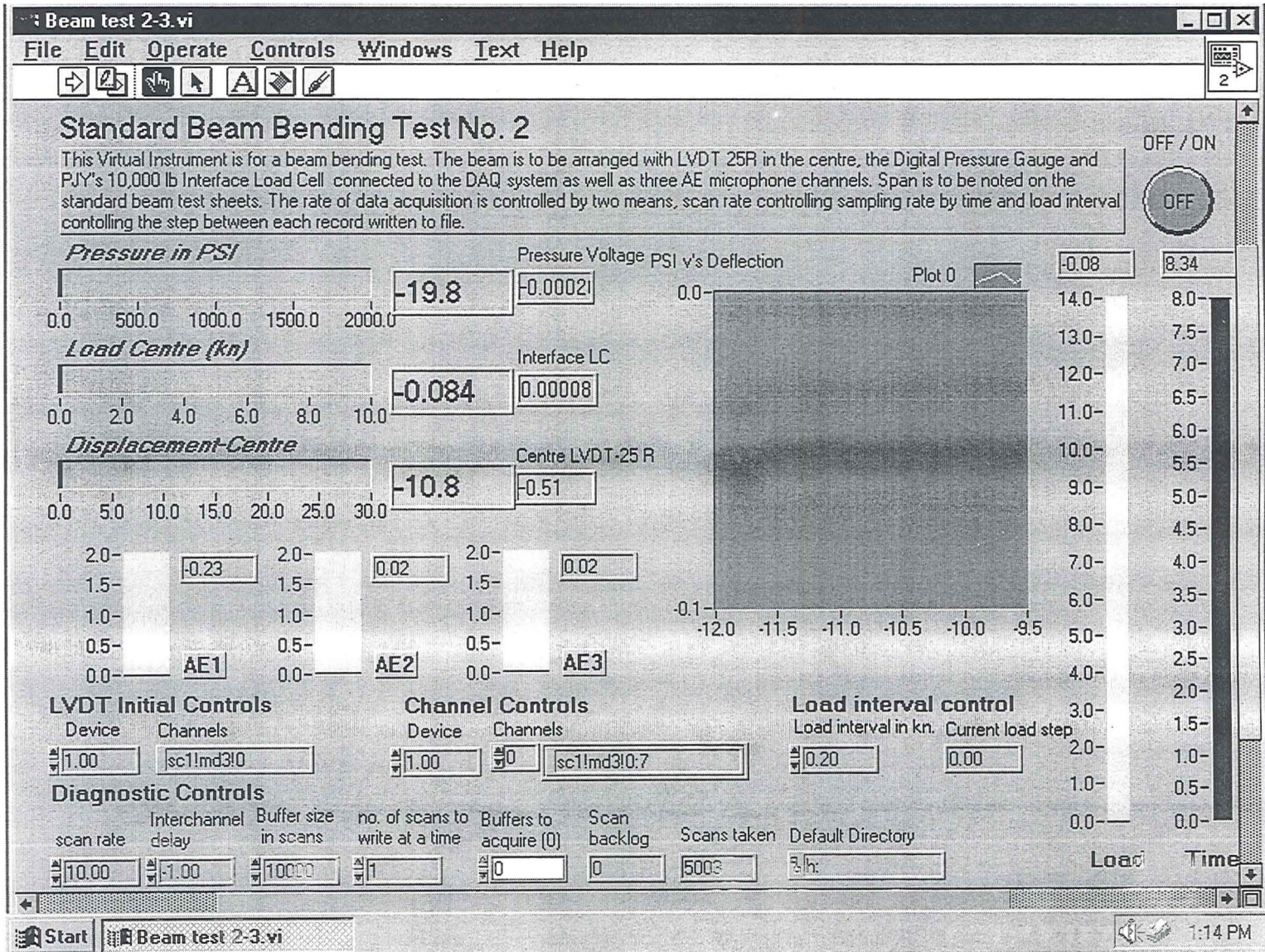
To save some space this has been rotated 90°. Here we gather all information, which will make it possible to write to a file so we can save it. The arrow to the right gets the data in different columns and the left arrow indicates End of file.

17



By dividing the scans taken by 600 we continuously get the time in minutes for how long the program has been running.

Figure A.1
The Panel window of Beam test 2-3. vi.



A6



Appendix A





Appendix A

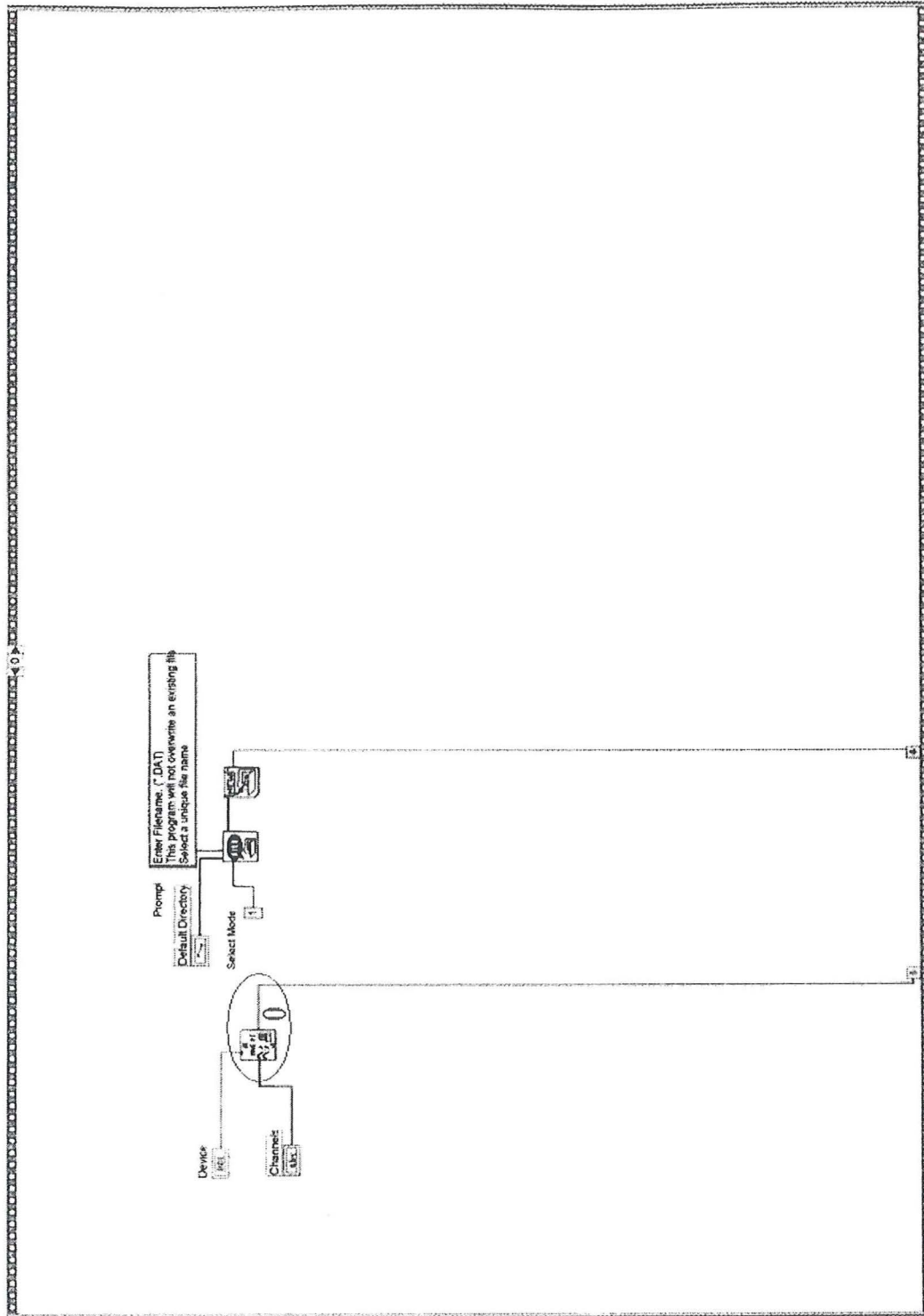


Figure A.2
The Diagram window's frame number 0 of Beam test 2-3.vi.



Appendix A

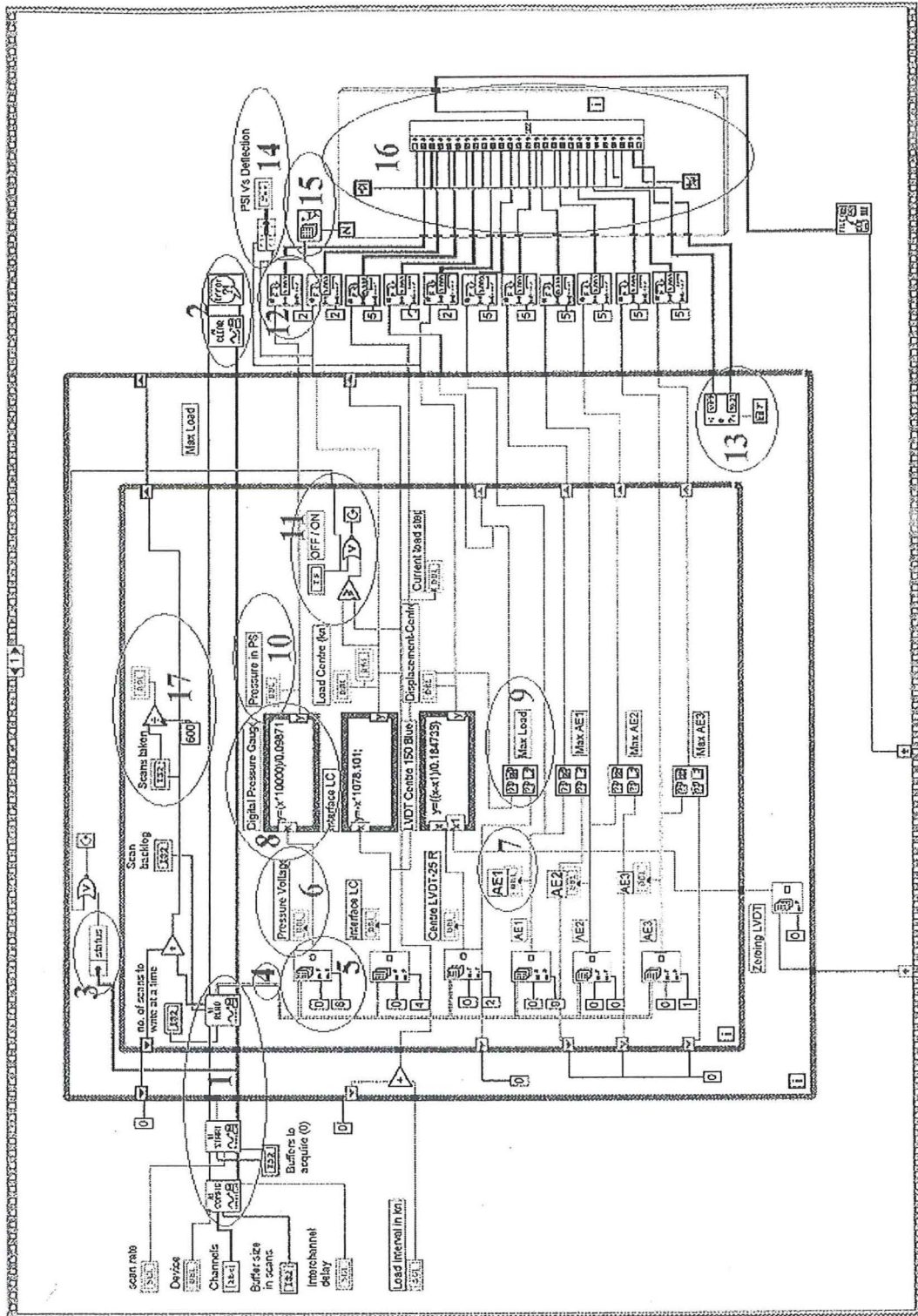


Figure A.3
The Diagram window's frame number 1 of Beam test 2-3.vi.



Appendix A

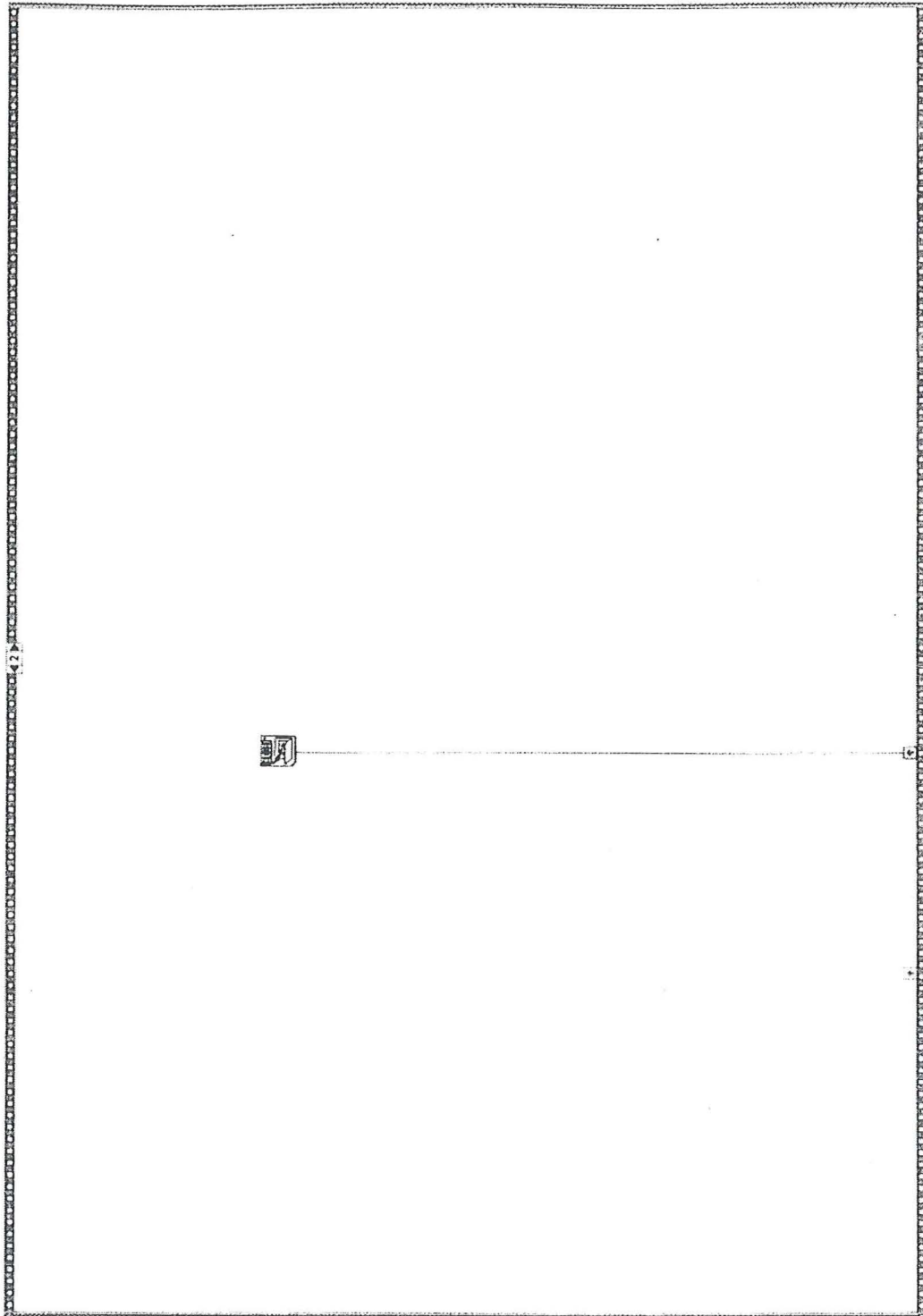


Figure A.4
The Diagram window's frame number 2 of Beam test 2-3.vi.



Appendix B



Comparison between AE1 and AE2

The need for not using the clamp

As described in 6.1 The setup two sensors, AE1 and AE3, were attached to the beam with a clamp, and AE2 was put directly under one of the load points. The problem was that when the beam broke it splintered and thereby the depth of the beam became greater, causing pressure on the sensors. Even the bar of the clamp got warped. Because of this the sensors did not get very good contact with the beam. It was like a small wedge of air between them. The bar was straightened a pair of times, so the test could continue only to see it getting warped again. On top of this the sensors did not seem to handle the exposed force when the beam splintered very well. The top of the case got damaged and the signals from AE3 started to look a bit strange.

It all added up to three major problems. We were destroying sensors and that could definitely not continue. The results we got were not really reliable, as we could not trust that there was sufficient acoustic coupling between the beam and the sensors. The attachment of the clamp and especially that it had to be straightened about every fourth test or so was very time consuming. A way to collect the information without using the clamp was necessary.

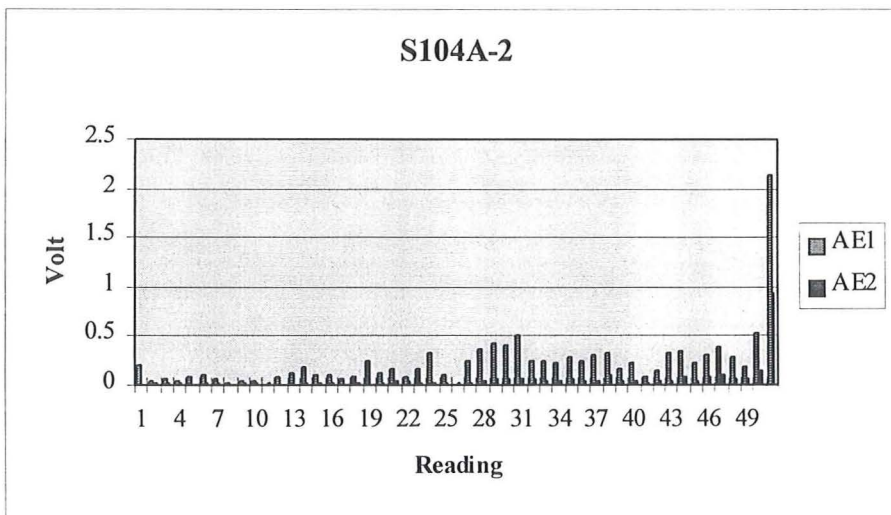
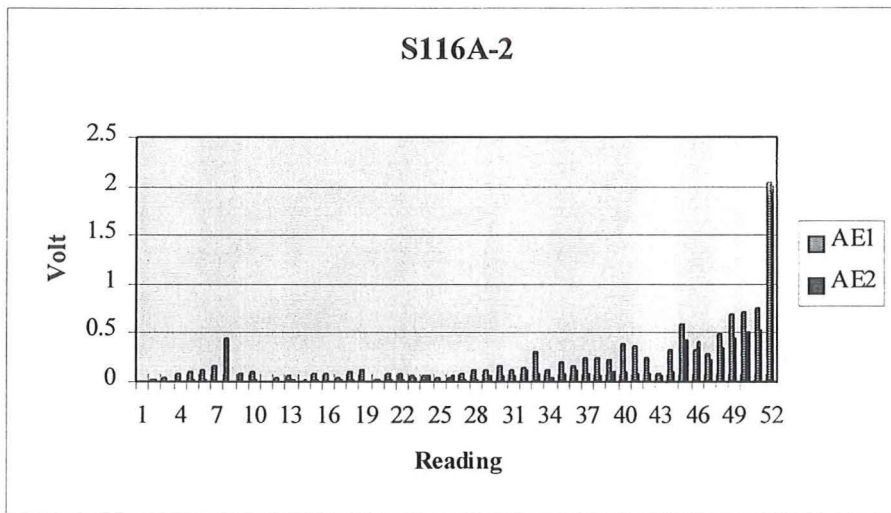
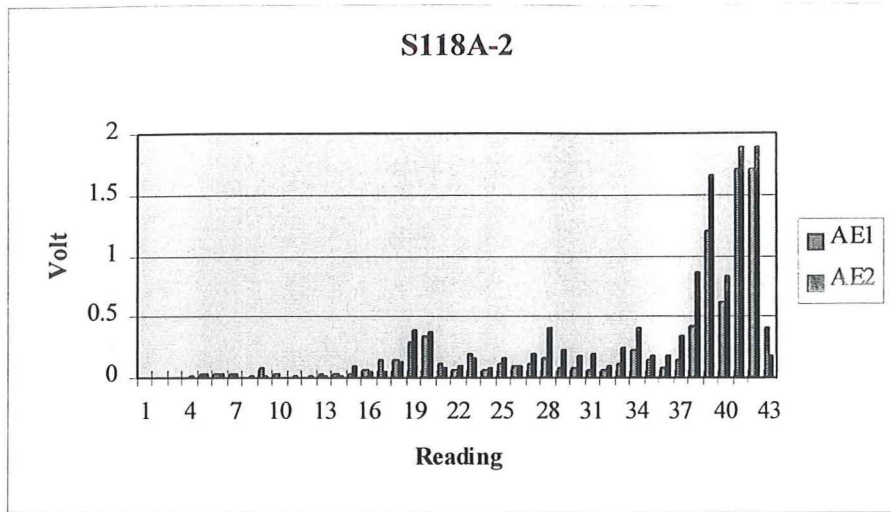
Comparing AE1 and AE2

To try and solve the problems I compared the data from AE1 and AE2 to see if the pattern and the trend were the same. Until then ten samples had been tested. The diagrams of these are seen on the following pages in the same order they were tested.

The pattern, trend and level of voltage corresponds very well for S118A-2, S116A-2, S108A-2 and S99A-2. For S104A-2, S103A-2 and S109A-2 the pattern and the trend are mainly the same, while the voltage differs a bit more. For S100A-2 AE1 is hardly noticeable. The last two, S97A-2 and S117A-2, have less correspondence, but still not too bad. It is clear that AE2 is able to register the acoustic emissions from the beam. For AE1 and AE3 there is always the question of good acoustic coupling or not. Was there enough grease when attached? Is there an air wedge? These two questions reveal a great deal of uncertainty about the acoustic coupling for AE1 and AE3. That does not go for AE2, which stays in the same place for all tests. I got to the conclusion that AE2 is just as good, if not even a more reliable source for the purpose of this research compared to AE1 and AE3. I discussed the issue with Dr Doe and he had the same opinion. It was then decided to abandon the use of the clamp and stick to AE2. To get as much information as possible from the test AE3 was moved and placed in the same way as AE2 under the other load point. AE3 had been changed into an undamaged sensor before it was moved.

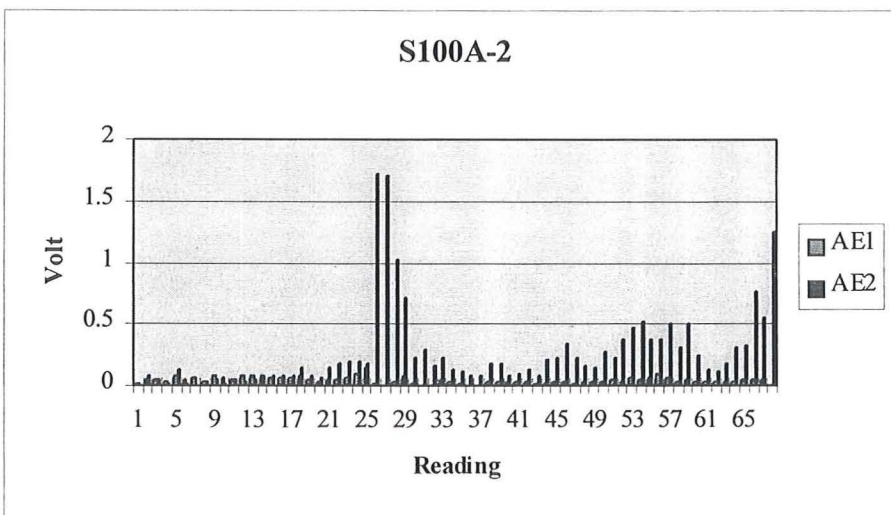
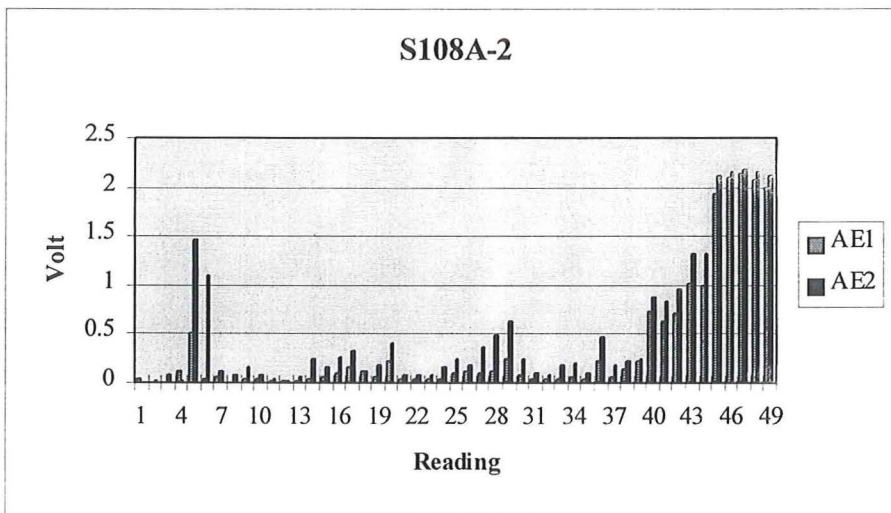
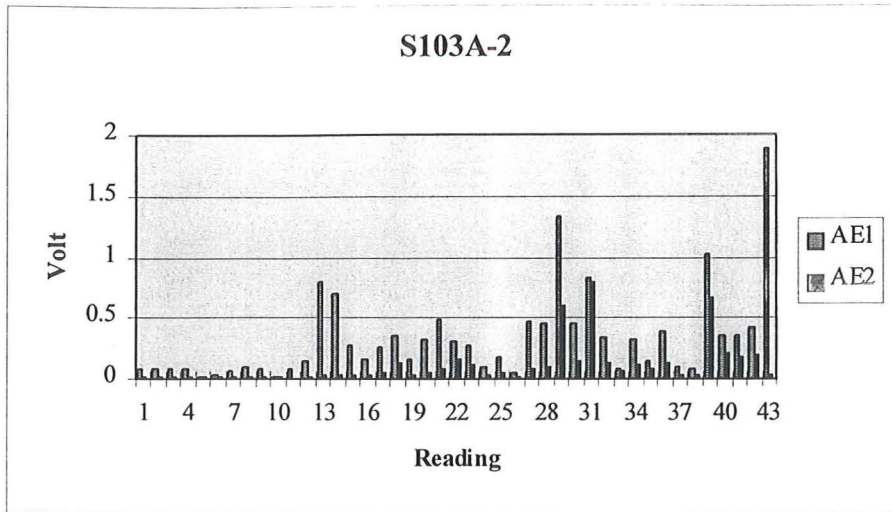


Appendix B



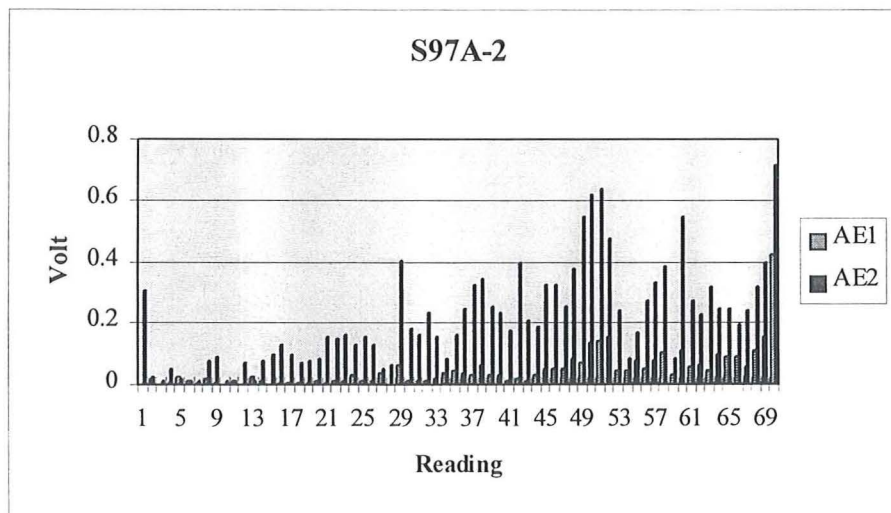
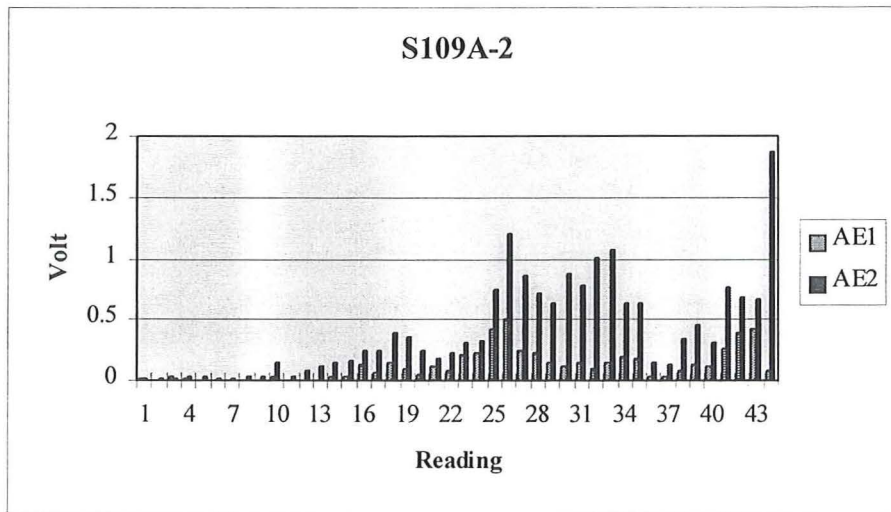
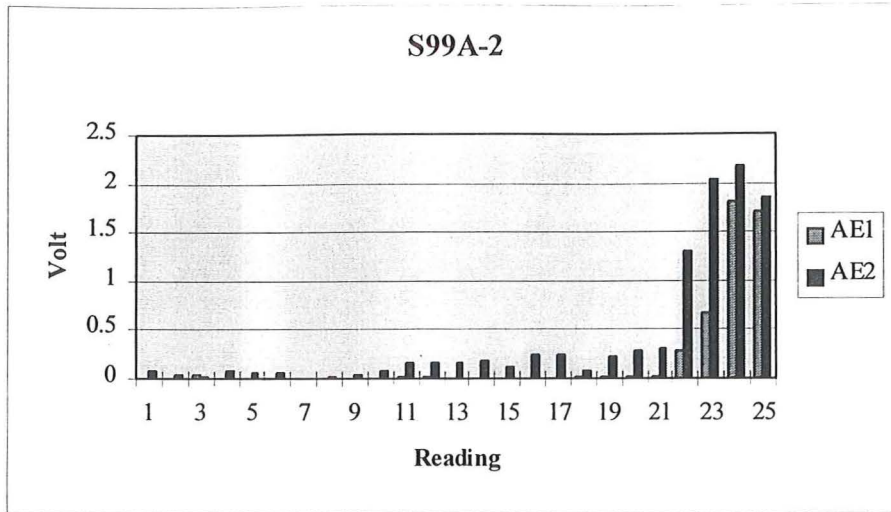


Appendix B



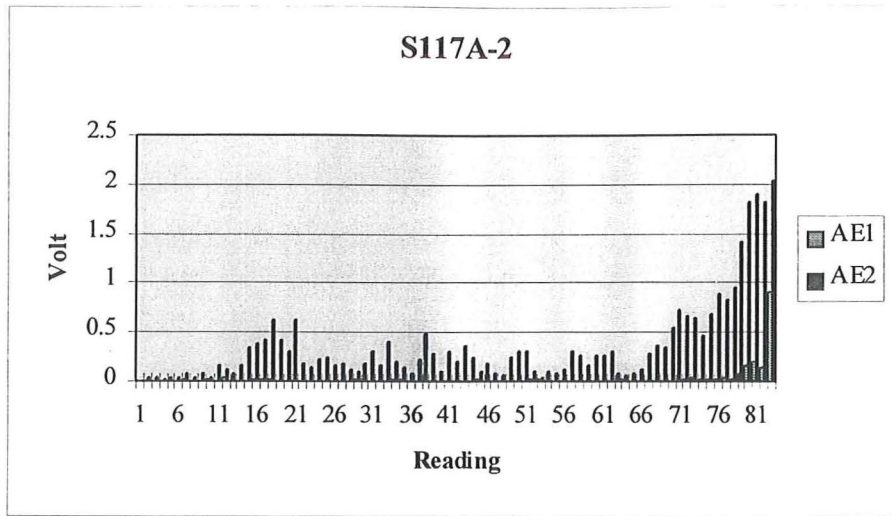


Appendix B





Appendix B





Appendix C



Explanation of the data

The comments in this appendix refer to Table C.1 on the next page. The reason for choosing T177A-2 had only to do with the fact that it fitted well to one page. The data is presented in the same way as when opened as an Excel file, with a pair of exceptions. Headings have been added at the bottom of each column and to make it more readable. Grid lines have also been added. When opened Excel adapts the same file name, in this case T177A-2. This is not visible in Table C.1, but is of course very useful when it comes to the capability of separating different tests.

The first two columns show the load in Pressure per Square Inch (PSI) respective in kilo Newtons (kN). A reading of the load is taken at each load step of 0.2 kN. In this case the beam was unloaded somewhere between 5.41 kN and 5.61 kN. Because of this the number in the last cell of the column look a bit strange.

In the next column is the voltage (V) of the load cell. The voltage is transformed into PSI and kN with the formulas used by Beam test 2-3.vi, see Appendix A.

The values in the column marked Max load are the maximum load for each interval. As the interval load and the maximum load for the interval are the same until the last reading, the second and fourth column looks very much the same. Only the last reading is different. The value 5.47 kN is the ultimate load this beam could take.

The next column contains the deflection in mm. It does not start from zero. When calculating the elasticity it is the relative deflection to load that is interesting, so the fact that the deflection does not start from zero does not matter.

The following two columns for AE1 are not relevant at all, as this sensor was not connected.

The data for AE2 and AE3 in volt are in the same way as for the load. One column for the AE at the load step and the other column for the maximum AE in the interval.

In the last two columns are the date and time for each reading. This way the tests can be sorted in the order they were performed. If some results are a bit strange it can be checked if anything special happened during those tests, or if there is a completely new trend this might be traced to some event that changed how the test was carried out. To have the actual time for every reading gives the possibility to get the actual load rate, which is highly interesting.



Appendix C



29.68	0.21	-0.0002	0.21	0.5	-0.2002	0	0.0293	0.44434	0.02441	0.05859	10/18/96	4:10:47 PM
59.36	0.4	-0.00037	0.4	1.16	-0.20508	0	0.01465	0.08789	0.01465	0.05371	10/18/96	4:10:53 PM
79.14	0.61	-0.00057	0.61	1.9	-0.21484	0	0.07324	0.11719	0.01465	0.04883	10/18/96	4:11:06 PM
89.03	0.8	-0.00074	0.8	2.54	-0.21973	0	0.04883	0.08301	0.00977	0.04395	10/18/96	4:11:31 PM
128.6	1.01	-0.00094	1.01	3.33	-0.20996	0	0.0293	0.08301	0.02441	0.05371	10/18/96	4:11:42 PM
138.5	1.2	-0.00111	1.2	4.04	-0.20996	0	0.04395	0.07324	0.0293	0.05371	10/18/96	4:11:59 PM
158.28	1.41	-0.00131	1.41	4.81	-0.21484	0	0	0.04883	-0.00977	0.0293	10/18/96	4:12:03 PM
178.07	1.6	-0.00148	1.6	5.63	-0.20996	0	0.0293	0.03906	0.0293	0.03418	10/18/96	4:12:05 PM
207.75	1.81	-0.00168	1.81	6.32	-0.20508	0	0.03418	0.09277	0.0293	0.04395	10/18/96	4:12:06 PM
217.64	2	-0.00186	2	7.03	-0.20996	0	0.06348	0.09277	0.01953	0.04883	10/18/96	4:12:10 PM
237.42	2.21	-0.00205	2.21	7.72	-0.20508	0	0.03906	0.09277	0.00488	0.04883	10/18/96	4:12:12 PM
257.21	2.4	-0.00223	2.4	8.43	-0.20508	0	0.04883	0.08301	0.0293	0.04883	10/18/96	4:12:18 PM
286.89	2.61	-0.00242	2.61	9.17	-0.19531	0	0.09277	0.12207	0.03418	0.04395	10/18/96	4:12:25 PM
306.67	2.8	-0.0026	2.8	9.89	-0.19043	0	0.22949	0.28809	0.07324	0.07813	10/18/96	4:12:32 PM
336.35	3.01	-0.00279	3.01	10.73	-0.18555	0	0.19043	0.25391	0.00977	0.05371	10/18/96	4:12:38 PM
346.24	3.2	-0.00297	3.2	-28.6	-0.20996	0	0.23926	0.44922	0.03906	0.15137	10/18/96	4:12:47 PM
366.03	3.41	-0.00316	3.41	-28.55	-0.23926	0	0.30762	0.31738	0.03418	0.06348	10/18/96	4:12:58 PM
395.71	3.6	-0.00334	3.6	-28.55	-0.26367	0	0.38574	0.39551	0.03418	0.07324	10/18/96	4:13:03 PM
415.49	3.81	-0.00354	3.81	-28.55	-0.29297	0	0.25391	0.46875	0.08301	0.08789	10/18/96	4:13:08 PM
445.17	4	-0.00371	4	-28.55	-0.3125	0	0.40527	0.4834	0.13672	0.13672	10/18/96	4:13:17 PM
445.17	4.21	-0.00391	4.21	-28.55	-0.33691	0	0.41016	0.60059	0.06836	0.15625	10/18/96	4:13:24 PM
474.85	4.4	-0.00408	4.4	-28.55	-0.36621	0	0.50781	0.85449	0.05859	0.18555	10/18/96	4:13:32 PM
504.52	4.61	-0.00428	4.61	-28.57	-0.39551	0	0.85449	1.13281	0.09766	0.34668	10/18/96	4:13:41 PM
524.31	4.8	-0.00445	4.8	-28.57	-0.42969	0	0.39063	0.86914	0.07324	0.19043	10/18/96	4:13:51 PM
553.99	5.01	-0.00465	5.01	-28.57	-0.44434	0	1.63086	1.85059	0.24902	0.71777	10/18/96	4:14:08 PM
563.88	5.2	-0.00482	5.2	-28.57	-0.44434	0	1.41602	1.64551	0.14648	0.27832	10/18/96	4:14:18 PM
583.67	5.41	-0.00502	5.41	-28.55	-0.44922	0	2.05078	2.07031	0.52246	0.54199	10/18/96	4:14:21 PM
-9.89	-0.02	0.00002	5.47	-28.76	-0.47363	0	0.66895	2.05566	0.05371	1.29395	10/18/96	4:14:25 PM
Load PSI	Load kN	Load cell voltage V	Max load kN	Deflection mm	AE1 V	AE1 Max V	AE2 V	AE2 Max V	AE3 V	AE3 Max V	Date	Time

Table C.1
The data of T177A-2. Except for headings and grid lines presented in the same way as opened in Excel.



Appendix D



Data used in the analysis

Data for sample distributions

The ultimate load was extracted from all successful tests. It was then sorted in bins of 1 kN to get the frequency for the histogram. The normal mass distribution was calculated for the mean of each bin with the following equation (19),

$$\text{Normal mass distribution } f(x) = \frac{1}{\sqrt{2 \times \pi \times S_x^2}} \times e^{-\frac{(x-X_m)^2}{2 \times S_x^2}} \quad \text{Equation D.1}$$

where S_x is the estimated population standard deviation, Equation 6.2
 X_m is the arithmetic mean, Equation 6.1

The data used is tabulated in Table D.1.

Scottsdale		
Load kN Bin	Frequency	Normal mass distribution
4.5	1	0.031264
5.5	5	0.044929
6.5	3	0.060449
7.5	6	0.076139
8.5	10	0.089783
9.5	8	0.099117
10.5	6	0.102439
11.5	4	0.099117
12.5	5	0.089783
13.5	11	0.076139
14.5	2	0.060449
15.5	1	0.044929
16.5	2	0.031264

Tarpeena		
Load kN Bin	Frequency	Normal mass distribution
2.5	1	0.039945
3.5	0	0.043386
4.5	8	0.046352
5.5	7	0.048708
6.5	8	0.050345
7.5	11	0.051184
8.5	14	0.051184
9.5	16	0.050345
10.5	9	0.048708
11.5	10	0.046352
12.5	2	0.043386
13.5	5	0.039945

Table D.1
 The data for the load histograms and normal mass distribution for Scottsdale and Tarpeena.

Data for AE2 Max analysis for Tarpeena

The data used for the AE2 Max analysis is tabulated in Table D.2a-d. In the first column is the sample number in the same order they were tested. The column Max load is the load at rupture for each test. MOR and MOE have been calculated from the results of each test with the following equation (9),



Appendix D



$$\text{Modulus of Rupture } MOR = \frac{3 \times P \times a}{b \times d^2} \text{ Pa}$$

Equation D.2

where P is the maximum load
a is the distance between supports and loading points
b is the breadth of the beam
d is the depth of the beam

$$\text{Modulus of Elasticity } MOE = \frac{L^3}{4 \times b \times d^3} \times \frac{P}{\Delta} \text{ Pa}$$

Equation D.3

where L is the span
b is the breadth of the beam
d is the depth of the beam
P is the load used during grading
 Δ is the deflection during grading

Ultimate reading is the reading corresponding to the load at rupture. In the next column is the reading when AE2 Max first reached 0.6 V. Note that because of the initial noise due to settling of the load the first 10 readings were not regarded. In the last column is the used capacity when AE2 Max first reached 0.6 V.



Appendix D



Sample number	Max load (kN)	MOR (Mpa)	MOE (Mpa)	Ultimate reading	Reading when AE2 Max > 0.6V	% of Max load when AE2 Max > 0.6V
T178A-2	9.52	54.4	11745	47	43	91%
T151A-2	8.32	47.5	16268	42	31	74%
T184A-2	8.63	49.3	10973	44	44	100%
T198A-2	5.18	29.6	12062	26	26	100%
T164A-2	8.38	47.9	12475	42	30	71%
T187A-2	4.04	23.1	8713	21	18	86%
T160A-2	8.68	49.6	10563	44	18	41%
T169A-2	5.31	30.3	12028	27	27	100%
T174A-2	7.88	45.0	13453	40	39	98%
T200A-2	10.25	58.6	11419	52	52	100%
T195A-2	7.08	40.5	12125	36	28	78%
T193A-2	4.91	28.1	9182	25	25	100%
T146A-2	7.41	42.3	12683	38	38	100%
T161A-2	11.90	68.0	13743	60	55	92%
T188A-2	7.77	44.4	12645	39	39	100%
T192A-2	13.20	75.4	13653	67	54	81%
T196A-2	9.14	52.2	10770	46	44	96%
T186A-2	2.72	15.5	7465	14	12	86%
T189A-2	7.01	40.1	11004	36	16	44%
T175A-2	11.67	66.7	13376	59	51	86%
T145A-2	9.69	55.4	13755	49	49	100%
T108A-2	6.49	37.1	10873	33	18	55%
T106A-2	8.21	46.9	12435	42	26	62%
T183A-2	7.08	40.5	10350	36	20	56%
T194A-2	5.73	32.7	11790	29	26	90%
T199A-2	11.58	66.2	12931	58	19	33%
T190A-2	6.91	39.5	10973	35	33	94%
T111A-2	9.98	57.0	11435	50	40	80%
T129A-2	9.96	56.9	14911	50	20	40%
Sample number	Max load (kN)	MOR (MPa)	MOE (Mpa)	Ultimate reading	Reading when AE2 Max > 0.6V	% of Max load when AE2 Max > 0.6V

Table D.2a
Data for AE2 Max analysis for Tarpeena. Test 1-29



Appendix D



Sample number	Max load (kN)	MOR (Mpa)	MOE (Mpa)	Ultimate reading	Reading when AE2 Max > 0.6V	% of Max load when AE2 Max > 0.6V
T124A-2	10.40	59.4	13103	53	25	47%
T109A-2	4.91	28.1	12588	24	20	83%
T107A-2	6.11	34.9	11405	31	19	61%
T172A-2	4.95	28.3	10214	25	25	100%
T177A-2	5.47	31.3	11361	27	21	78%
T182A-2	5.41	30.9	12426	28	18	64%
T110A-2	8.86	50.6	11083	45	17	38%
T112A-2	6.67	38.1	11346	34	19	56%
T136A-2	6.11	34.9	10590	31	11	35%
T118A-2	5.26	30.1	10829	27	24	89%
T117A-2	10.04	57.4	12632	51	30	59%
T171A-2	7.58	43.3	14617	38	30	79%
T166A-2	9.26	52.9	14277	47	27	57%
T122A-2	8.93	51.0	11838	45	34	76%
T135A-2	13.14	75.1	12811	65	53	82%
T162A-2	9.92	56.7	12025	50	36	72%
T197A-2	4.80	27.4	11967	25	21	84%
T143A-2	12.13	69.3	12435	61	54	89%
T133A-2	9.39	53.7	14288	47	24	51%
T139A-2	9.31	53.2	12830	47	40	85%
T185A-2	11.18	63.9	13100	56	46	82%
T191A-2	10.47	59.8	13711	53	32	60%
T132A-2	11.22	64.1	12257	57	17	30%
T105A-2	8.06	46.1	9867	41	15	37%
T168A-2	8.97	51.3	12462	45	24	53%
T116A-2	6.15	35.1	13300	31	23	74%
T181A-2	10.97	62.7	12150	55	32	58%
T154A-2	4.76	27.2	10232	23	22	96%
T138A-2	11.73	67.0	11081	59	26	44%
Sample number	Max load (kN)	MOR (MPa)	MOE (Mpa)	Ultimate reading	Reading when AE2 Max > 0.6V	% of Max load when AE2 Max > 0.6V

Table D.2b
Data for AE2 Max analysis for Tarpeena. Test 30-58



Appendix D



Sample number	Max load (kN)	MOR (Mpa)	MOE (Mpa)	Ultimate reading	Reading when AE2 Max > 0.6V	% of Max load when AE2 Max > 0.6V
T131A-2	8.09	46.2	10414	41	25	61%
T153A-2	11.33	64.7	13407	57	46	81%
T163A-2	11.14	63.7	12103	55	17	31%
T101A-2	4.80	27.4	10241	25	19	76%
T102A-2	8.76	50.1	12135	44	30	68%
T176A-2	8.13	46.5	11770	41	17	41%
T137A-2	7.54	43.1	12551	38	20	53%
T130A-2	9.12	52.1	14411	46	30	65%
T167A-2	7.29	41.7	12417	37	32	86%
T158A-2	9.54	54.5	11711	48	26	54%
T148A-2	9.67	55.3	13411	49	49	100%
T120A-2	6.67	38.1	11998	34	34	100%
T140A-2	9.98	57.0	12596	50	25	50%
T104A-2	7.81	44.6	10973	40	17	42%
T127A-2	10.36	59.2	10952	52	42	81%
T123A-2	11.56	66.1	11432	57	29	51%
T114A-2	5.29	30.2	10489	27	25	93%
T141A-2	10.21	58.3	11004	52	19	37%
T147A-2	9.92	56.7	10797	50	49	98%
T126A-2	8.93	51.0	10414	45	28	62%
T134A-2	9.62	55.0	13439	49	30	61%
T180A-2	9.41	53.8	12207	48	48	100%
T121A-2	13.83	79.0	11890	70	24	34%
T119A-2	7.35	42.0	11621	37	27	73%
T113A-2	10.84	61.9	12053	55	43	78%
T157A-2	6.53	37.3	11235	33	28	85%
T125A-2	12.42	71.0	11857	63	63	100%
T152A-2	13.67	78.1	11514	69	54	80%
T103A-2	4.46	25.5	18617	23	15	65%
Sample number	Max load (kN)	MOR (MPa)	MOE (Mpa)	Ultimate reading	Reading when AE2 Max > 0.6V	% of Max load when AE2 Max > 0.6V

Table D.2c
Data for AE2 Max analysis for Tarpeena. Test 59-87



Appendix D



Sample number	Max load (kN)	MOR (Mpa)	MOE (Mpa)	Ultimate reading	Reading when AE2 Max > 0.6V	% of Max load when AE2 Max > 0.6V
T149A-2	8.93	51.0	13255	45	45	100%
T144A-2	13.60	77.7	13018	68	53	78%
T115A-2	11.48	65.6	12297	58	51	88%
T142A-2	10.84	61.9	11483	55	49	89%
Sample number	Max load (kN)	MOR (MPA)	MOE (Mpa)	Ultimate reading	Reading when AE2 Max > 0.6V	% of Max load when AE2 Max > 0.6V

Table D 2d
Data for AE2 Max analysis for Tarpeena. Test 88-91



References



References

- (1) Pearson R. G., Kloot N. H., Boyd J. D.
Timber Engineering Design Handbook
Melbourne 1958
- (2) Siau John F.
Transport Processes in Wood
New York 1984
- (3) National Association of Forest Industries
URL <http://www.nafi.com.au>
- (4) Tasmanian Timber Promotion Board
Tasmanian radiata pine (Undated)
- (5) Primary Industries South Australia
URL http://www.pi.sa.gov.au/pi_pub/factshts/farmfors.htm
- (6) The Information Resource for the Woodworking Industry
URL <http://www.woodweb.com/~treetalk/radiatapine.html>
- (7) Wilcox W. Wayne, Botsai Elmer E., Kubler Hans
Wood as a building material. A guide for designers and builders
New York 1991
- (8) Mårtensson A., Arfvidsson J., Dahlblom O.
Egenspänningar, sprickbildning och kupning vid virkestorkning Inledande studie
Lund 1992
- (9) Australian Standard 1720.1-1988
- (10) Physical Acoustics Corporation
URL <http://www.pacndt.com>
- (11) Adams R. D.
Fracture Development in Wood Resulting from Bending Stresses and Detected
Using the Acoustic Emission Phenomenon
Vancouver 1969



References



- (12) Sato K., Okano T., Asano I., Fushitani M.
Application of AE to Mechanical Testing of Wood
Lake Tahoe 1985
- (13) Physical Acoustics Corporation
Product specifications 1991
- (14) Standards Australia / New Zealand AS / NZS 4063:1992
- (15) Lawrence S. Aft
Fundamentals of Industrial Quality Control
Reading 1986
- (16) Henry E. Klugh
Statistics : The Essentials for Research
New York 1970
- (17) Doe Peter E.
Unpublished 1994
- (18) Meyer Stuart L.
Data Analysis For Scientists And Engineers
New York 1975
- (19) Hoel Paul G.
Introduction to Mathematical Statistics
New York 1954
- (20) National Instruments
LabVIEW Tutorial for Windows
1994